VOLUME 82 NUMBER 5

THE ASTROPHYSICAL JOURNAL

AN INTERNATIONAL REVIEW OF SPECTROSCOPY AND ASTRONOMICAL PHYSICS

Founded in 1895 by GEORGE E. HALE *and* JAMES E. KEELER

Edited by

DECEMBER 1935

THE UNIVERSITY OF CHICAGO PRESS
CHICAGO, ILLINOIS, U.S.A.

December 1935 Vol. 82, No. 5

THE ASTROPHYSICAL JOURNAL

AN INTERNATIONAL REVIEW OF SPECTROSCOPY AND ASTRONOMICAL PHYSICS

The Astrophysical Journal is published by the University of Chicago at the University of Chicago Press, 5750 Ellis Avenue, Chicago, Illinois, during each month except February and August. ¶ The subscription price is $6.00 a year; the price of single copies is 75 cents. Orders for service of less than a half-year will be charged at the single-copy rate. ¶ Postage is prepaid by the publishers on all orders from the United States, Mexico, Cuba, Porto Rico, Panama Canal Zone, Republic of Panama, Dominican Republic, Canary Islands, El Salvador, Argentina, Bolivia, Brazil, Colombia, Chile, Costa Rica, Ecuador, Guatemala, Honduras, Nicaragua, Peru, Hayti, Uruguay, Paraguay, Hawaiian Islands, Philippine Islands, Guam, Samoan Islands, Balearic Islands, Spain, and Venezuela. ¶ Postage is charged extra as follows: for Canada and Newfoundland, 30 cents on annual subscriptions (total $6.30); on single copies, 3 cents (total 78 cents); for all other countries in the Postal Union, 80 cents on annual subscriptions (total $6.80), on single copies, 8 cents (total 83 cents). ¶ Patrons are requested to make all remittances payable to The University of Chicago Press, in postal or express money orders or bank drafts.

The following are authorized agents:

For the British Empire, except North America, India, and Australasia: The Cambridge University Press, Fetter Lane, London, E.C. 4. Prices of yearly subscriptions and of single copies may be had on application.

For Japan: The Maruzen Company, Ltd., Tokyo.

For China: The Commercial Press, Ltd., 211 Honan Road, Shanghai. Yearly subscriptions, $6.00; single copies, 75 cents, or their equivalents in Chinese money. Postage extra, on yearly subscriptions 80 cents, on single copies 8 cents.

Claims for missing numbers should be made within the month following the regular month of publication. The publishers expect to supply missing numbers free only when losses have been sustained in transit, and when the reserve stock will permit.

Business correspondence should be addressed to The University of Chicago Press, Chicago, Illinois.

Communications for the editors and manuscripts should be addressed to: Otto Struve, Editor of THE ASTROPHYSICAL JOURNAL, Yerkes Observatory, Williams Bay, Wisconsin.

The cable address is "Observatory, Williamsbay, Wisconsin."

The articles in this journal are indexed in the *International Index to Periodicals*, New York, N.Y.

Applications for permission to quote from this journal should be addressed to The University of Chicago Press, and will be freely granted.

Entered as second-class matter, January 17, 1895, at the Post-Office, Chicago, Ill., under the act of March 3, 1879.
Acceptance for mailing at special rate of postage provided for in Section 1103, Act of October 3, 1917, authorized on July 15, 1918.

PRINTED IN THE U.S.A.

THE ASTROPHYSICAL JOURNAL

AN INTERNATIONAL REVIEW OF SPECTROSCOPY AND ASTRONOMICAL PHYSICS

VOLUME 82 DECEMBER 1935 NUMBER 5

THE DISTRIBUTION OF CENTERS OF ATTRACTION FOR PROMINENCES

By PHILIP C. KEENAN

ABSTRACT

Measurement, on Yerkes spectroheliograms, of the heliographic latitudes of centers of influence for prominences shows that such centers are largely confined to the sun-spot zones. They exhibit a marked correlation with individual spots, though some centers are formed in regions entirely free from sun-spots. The zone of maximum frequency of occurrence of centers of attraction extends from the middle of a spot to slightly beyond the penumbra.

The centers themselves have diameters ranging from the limit of resolution up to 25,000 km, and they commonly attract prominences as far away as 50,000–200,000 km. For thirty-nine streamers the average mass velocity was measured as 51 km/sec. Double streamers were found in eighty-nine prominences.

As numerous observers have noted, active prominences on the sun are frequently characterized by long, curved streamers apparently terminating in disturbed regions of the chromosphere which often lie over or near sun-spots. In particular, F. Slocum called attention in 1912[1] to a large spot which attracted matter from prominences as far away as 260,000 km. J. Evershed,[2] on the other hand, observed a tendency for prominences to be ejected from spots. A more extended study of phenomena of this class was made by E. Pettit[3] in connection with his general investigation of the forms and motions of prominences. He concluded that, while brilliant jets are not infrequently thrown out from spots," . . . . normally

[1] *Ap. J.*, **36**, 265, 1912.

[2] *Mem. Kodaikanal Obs.*, **1**, Part 2, 93, 1917.

[3] *Pub. Yerkes Obs.*, **3**, 205, 1925.

the matter about the spot is moving into it with accelerated velocities averaging about 35 km/sec, sometimes reaching 100 km/sec." The occurrence of some centers of attraction in regions where no spot was observed was also noted specifically by him.

Statistical data are needed to bring out more clearly the relationship of sun-spots to the motions of the gases in the prominences around them, and it was as a step in this direction that Dr. Pettit suggested this study of the Yerkes collection of some ten thousand spectroheliograms extending over the interval from 1904 to 1935.

Heliographic latitudes to the nearest tenth of a degree were determined for all recognizable centers of influence, although the positions of many are so poorly defined as to be uncertain by as much as a degree. After a little experience in examining the plates, it was usually fairly easy to distinguish true lines of motion from those broader streamers, common especially in higher latitudes, which are relatively stable and exhibit no definite mass velocities. Nearly all doubtful cases were excluded. On many days the plates were insufficient in number or were taken too far apart in time to define the direction of motion, but, wherever possible, expulsion was indicated by a plus sign and attraction by a minus sign.

The latitude distribution of all observed centers of influence is given in Figure 1, where the abscissae represent the fraction of the current sun-spot period elapsed since the last previous minimum. The apparent concentration of the points at certain phases is due mainly to the greater number of plates in some years than in others, though the number of centers does unquestionably increase at the time of sun-spot maximum. While the work of many observers is represented in the material, the greater part of the observations included were made by Fox, Lee, Pettit, or Morgan and Higgs.

The diagram shows clearly that centers of activity are uncommon in high latitudes. Only 4 points out of 384 in the figure lie in latitudes greater than 70°, and the great majority are within 50° of the equator in spite of the fact that one of the two zones of maximum prominence activity is centered between 50° and 80°. The tendency to cluster along the latitudes of maximum frequency of sun-spots suggests a strong correlation between the presence of a spot and the development of a center of attraction. However, the dependence is

PLATE XIV

CENTERS OF ATTRACTION FOR NORMAL PROMINENCES

PLATE XV

1 2

3, 4 5

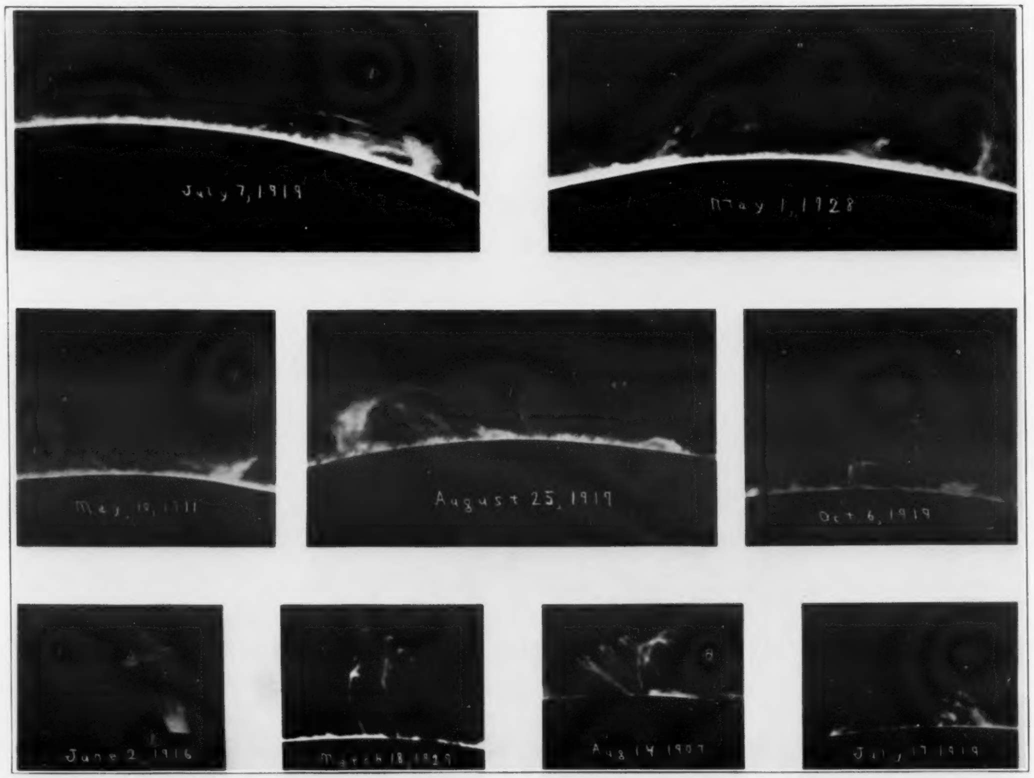

6 7 8 9

CENTERS OF ATTRACTION FOR SPOT PROMINENCES

not complete, for the scatter in Figure 1 is greater than in Maunder's "butterfly" diagram and tends to obscure the characteristic variation of latitude with phase.

Before the correlation is examined more closely, it is necessary to separate the material according to the type of prominence involved. We wish to know whether sun-spots accompany the growth of cen-

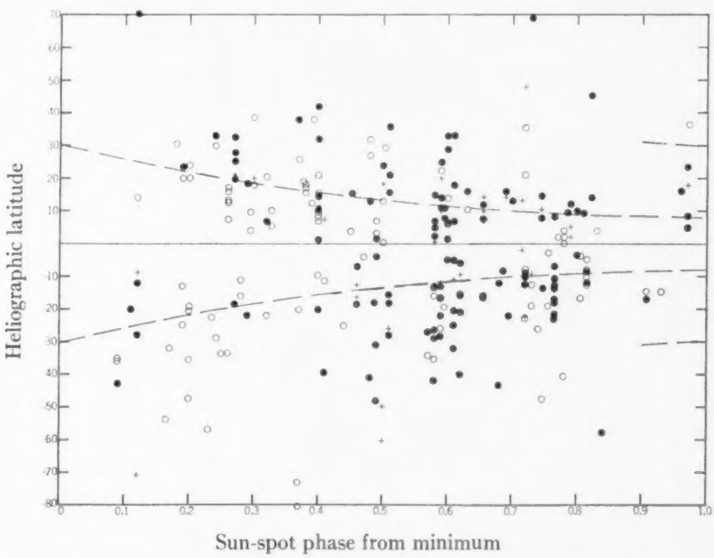

FIG. 1.—Latitude distribution of centers of motion. Filled circles indicate attraction and crosses expulsion. Open circles signify that the direction of motion was unknown.

ters of attraction for ordinary prominences which previously may have been either active or quiescent. The fountain, or spot, prominences of Pettit's classification[4] were therefore treated separately, since they almost invariably are part of the phenomena accompanying spot disturbances[5] and would introduce a misleading correlation if included with the independent prominences. It is usually not difficult to distinguish between the two types, as may be seen from the examples shown in Plates XIV and XV. The distinction between the two types is fundamental; radiating jets and the rarer complete loops are characteristic features of spot prominences.

[4] *Ap. J.*, **76**, 9, 1932.

[5] Cf. M. A. Evershed; *M.N.*, **73**, 422, 1913.

In Figure 2 are shown frequency diagrams giving the numbers of occurrences of centers of motion at given distances from the nearest sun-spot having a longitude within 20° of that of the limb

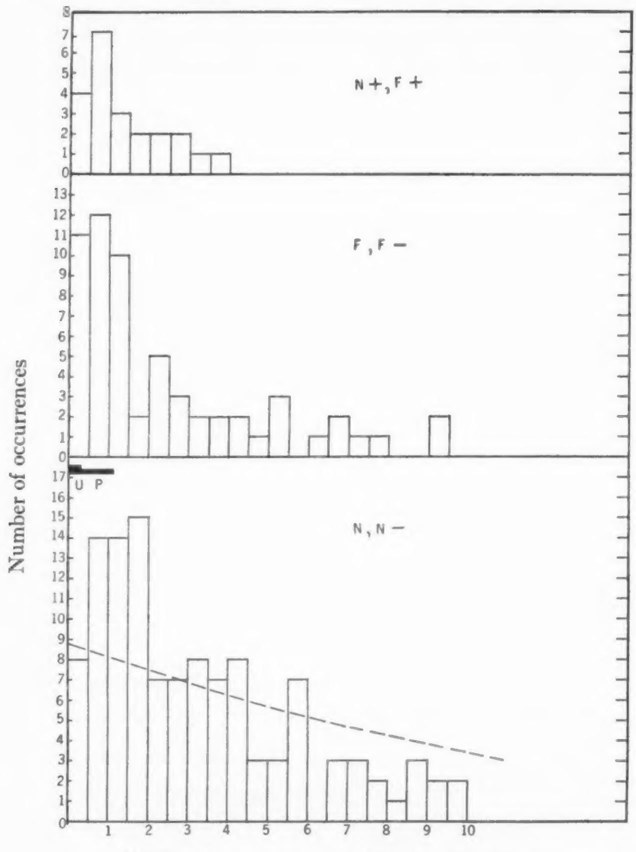

FIG. 2.—Frequency diagram of centers of motion as a function of distance from sun-spots. Cases of expulsion are collected in the upper section. Lower sections show distribution of attractive centers for fountain and normal prominences, respectively. Average radii of spot umbrae and penumbrae are marked above the letters *U* and *P*.

at the time of observation of the prominence. Very often it was necessary to use spot positions obtained from the Greenwich catalogues measured several days earlier or later than the prominence. While this was for the most part due to the difficulty of detecting

spots on the limb, there is reason to believe that centers of motion sometimes appear in advance of the formation, or after the dissolution, of sun-spots.

The upper diagram includes the relatively few cases of expulsion of matter. Since a great majority of the normal prominences, especially, showed motions toward the disk, there is probably little error introduced by including undetermined motions among the cases of attraction.

Consider particularly the normal prominences. In order to compare the observed distribution with that to be expected if the centers of attraction were scattered at random along the disk, we make use of the probability formulae given by Russell and Bowen[6] for the coincidences of arbitrary wave-lengths with spectral lines in a given range of spectrum, corresponding in our problem to the total range in latitude along one limb. The limits were taken as $\pm 50°$, since otherwise the concentration of points in low latitudes would produce an apparent excess of small distances regardless of whether there is any correlation with individual spots. Differentiation of equation (1) of the paper cited leads to the expression

$$\Delta p = \frac{-2M}{X}\left(1-\frac{2x}{X}\right)^{M-1}\Delta x ,$$

where Δp is the probability of occurrence of a minimum distance between x and $x + \Delta x$; X is the total arc of the limb taken into account, namely, 100°; and M is the average number of spots within the given distance from the limb on any one day, namely, 5.3.

Taking Δx as 0°.5 and multiplying by 166, the total number of centers of attraction for normal prominences, we obtain the broken line of the lower diagram of Figure 2. The greater the distance of any one spot from a center, the greater is the probability that it will be omitted from the count because of the presence of another spot closer to the center; consequently, the line of probability for chance coincidences slopes downward to the right.

If the observed frequencies are divided by the corresponding values for the broken line, we obtain the departure from uniform

[6] *Ap. J.*, **69**, 196, 1929.

distribution. The concentration within 2° of the center of spots is striking, particularly when it is recalled that the apparent frequency within a range Δx at any distance x is a summation of all prominences over a considerable spread in longitude, which has been taken as 20° (see Fig. 3). The observed number, $S(x)$, is related to

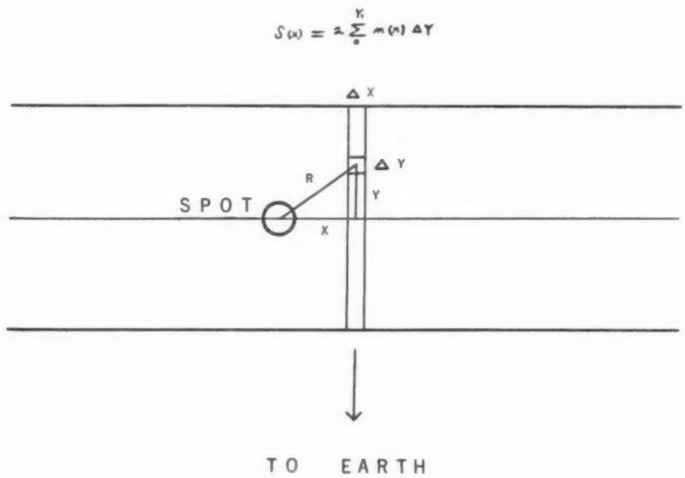

FIG. 3.—Section of sun's disk at limb as seen from above. The spot is assumed to lie on the limb.

the true distribution function $n(r)$ by an integral equation which may be written as the summation

$$S(x) = 2 \sum_{0}^{y_1} n(r) \Delta y \, .$$

There should probably be included some weighting factor diminishing with greater distances from the limb, but in any case, the data are not extensive enough to justify an attempt to compute $n(r)$ exactly. It is sufficient to notice that the smoothing effect is greatest at small distances from the middle of a spot, so that the observed hump corresponds to a real maximum which is much more pronounced but is not shifted along the x-axis to any great extent. The apparent dip at the very middle of the spots may be due to the inclination of some of the streamers at their intersection with the disk.

PLATE XVI

1 2 3

4, 5 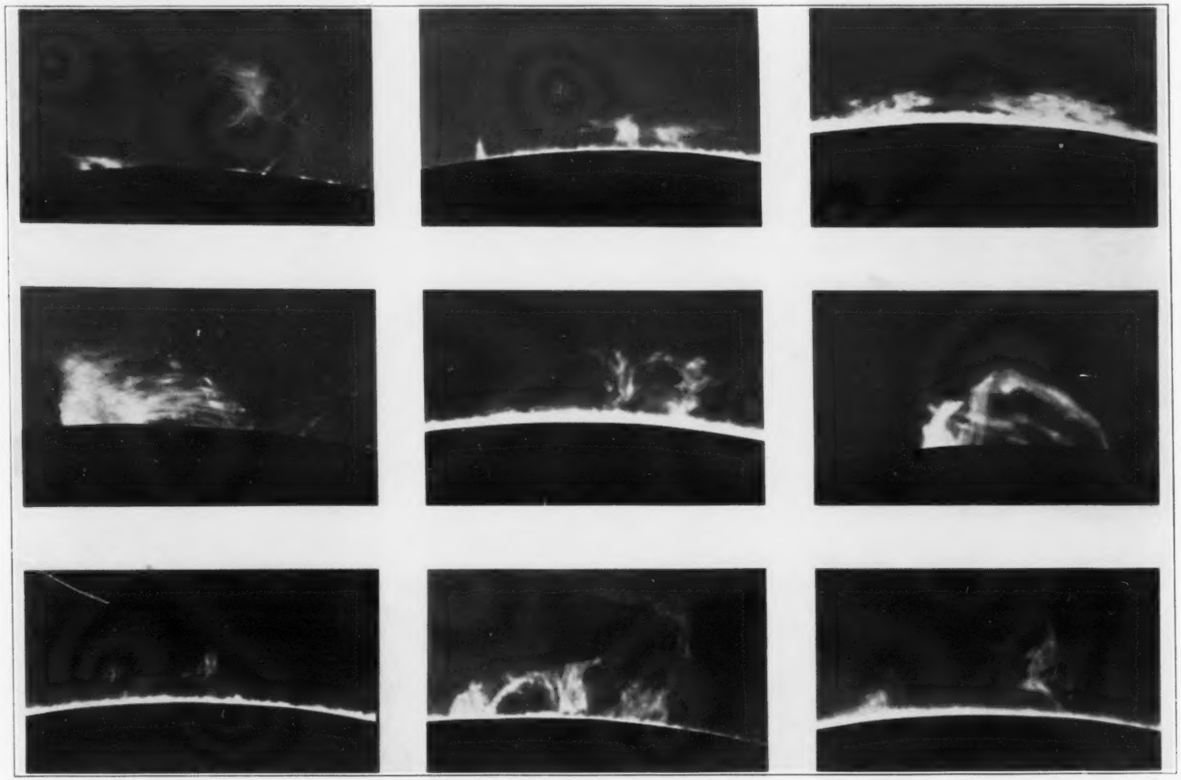 6

7 8 9

Prominences with Double Streamers

If the prominence is actually some distance away from the limb, the effect of projection will be an apparent shift outward. However, the inclination is usually so slight that the effect must be small. In any case, it may be concluded that there is a strong tendency for centers of motion to be associated with spots, and that the field of greatest attraction includes the penumbra and extends perhaps a quarter of its diameter outside. On the other hand, 28 out of the 166 centers of attraction for normal prominences were more than 10° from the nearest spot; consequently, the presence of an actual spot is not essential to their formation.

A measure of the extent of the influence of the centers of attraction is given by the greatest distance of prominences from which matter is definitely drawn. Usually this distance lies between 50,000 and 200,000 km, but is occasionally greater; the prominence of September 3, 1904, contained streamers covering an arc of more than 30°, or 360,000 km. The breadth of the centers themselves, as judged by the widths of the streamers at the point of contact with the limb, is probably often less than 5000 km and cannot be resolved on the plates; but a majority of them are larger, lying between 5000 and 25,000 km.

When several sequential plates were available, it was possible to estimate the mass velocities in the streamers from displacements of definite knots of matter. For 39 prominences measures near the point of attraction gave motions ranging from 3 to 190 km/sec, with 51 km/sec as the average, though both the slowest and the fastest probably escape measurement on the spectroheliograms.

An interesting by-product of the examination of the plates was a list of 89 prominences which exhibited double streamers—a feature which is therefore not rare and which has been noticed by others. Nine of the best examples are reproduced in Plate XVI, which is enlarged from negatives taken by Slocum, Lee, and Pettit.

The appearance of multiple streamers following a more or less parallel course is known to be common, and without doubt most of the double streamers merely represent such cases where the number of separate streamers happens to be two. This is probably true, for example, in Nos. 2 and 3 of the illustrations. However, the appearance of the prominences on several of our best plates suggests that

some of the apparently double streamers are actually single structures, which, in accordance with a suggestion made several years ago by Struve to explain the tendency of many prominences to be brighter at the edges than in the center, may have the form of a hollow tube. However, the observations could be described equally well by assuming that we have to do with pairs of parallel streamers which attract the matter from one to another so that the space between them is partly filled.

Additional evidence in favor of the interpretation of double filaments as unit structures, either tubular or ribbon-like, is furnished by the absorption which is occasionally shown when the streamers pass in front of other prominence material (see No. 1).

The measured separations of the double streamers vary from 2300 km to 14,000 km, with the majority lying between 5000 and 10,000 km apart. Prominence No. 4 belongs to a rather rare type in which there are numerous coarse streamers exhibiting a double "fine structure." It is possible that many cases of this sort escape observation, since unusually good observing conditions are required to resolve detail of this fineness, and still smaller separations may exist without our being able to detect them.

Preliminary examination of many of the plates was carried out by Mr. Paul Rudnick, while much of the work of reducing the observations and preparing the illustrations was done by Miss Edith Kellman.

YERKES OBSERVATORY
September 1935

RELATIVE *f*-VALUES FOR LINES OF *Fe* I FROM ELECTRIC-FURNACE ABSORPTION SPECTRA*

By ROBERT B. KING and ARTHUR S. KING

ABSTRACT

The total absorptions of lines of *Fe* I in furnace absorption spectra have been measured at a temperature of 2100° C, and the relative intensities of the lines at that temperature have been derived from the *linear* portion of the *curve of growth* of an absorption line where the total absorption $\propto Nf$. Variation of N, the number of atoms per cubic centimeter in the furnace, allows the study of a wide range of intensities. The condition of thermal equilibrium existing in the furnace permits the application of the Boltzmann formula to the observed relative intensities and gives the relative *f*-values of the line. Only the relative *f*-values are obtained, since the absolute value of N is unknown.

That the *linear* portion of the curve of growth affords a valid method of observation under these conditions is verified by comparison of the measured total absorptions of lines in five multiplets of *Ti* I with Harrison's measures of the relative intensities of these lines in the arc.

The condition of thermal equilibrium in the furnace is checked by observing the change in the intensities of *Fe* lines arising from different levels when the furnace temperature is raised from 1800° C to 2400° C.

Relative *f*-values are given for seventy-five lines in nine multiplets of *Fe* I of temperature classes I and II in the region λλ 3650–4400. The average probable error is about 8 per cent.

THE METHOD

An astrophysical problem of growing importance is the study of the "curve of growth"[1] of an absorption line in the solar and in stellar atmospheres. Notably, it has led to the elucidation of the so-called "gradient effect"[2] and to the postulation of turbulence in the atmospheres of certain stars.[3] Usually the *total absorptions* of multiplet components and the lines of overlapping multiplets, whose theoretical or laboratory intensities are known, are used to trace the course of the curve. A serious handicap to this work has been the scarcity of theoretical or laboratory data on the line intensities, especially in the complex spectra of the elements of the iron group. Because of their large number and great range in intensities, the lines of these elements are particularly suitable for studying the curve of growth.

* *Contributions from the Mount Wilson Observatory, Carnegie Institution of Washington*, No. 528.

[1] For general discussion and bibliography see Minnaert, *Observatory*, **57**, 328, 1934.

[2] Numerous articles by Struve, Elvey, Morgan, and Hynek, *Ap. J.*, 1930–34.

[3] Struve and Elvey, *Ap. J.*, **79**, 409, 1934.

In laboratory measurements of line intensities in complex spectra, the arc has usually been used as a source. While a relatively high degree of precision is possible in arc intensity measurements, the arc as a source has the disadvantages that self-reversal is troublesome, and usually no real temperature can be assigned to the excitation. In some cases[4] self-reversal may be largely eliminated or a correction applied; but the deviations from thermal equilibrium and the Boltzmann formula are even more serious[5] and give rise to grave uncertainties, especially when the lines under consideration arise from levels differing considerably in excitation potential.

The electric vacuum furnace has the great advantage that the atoms are in thermal equilibrium at a known temperature and that the Boltzmann formula may be applied to the observed intensities to reduce them to correspondence with a priori transition probabilities. At the beginning of this work attempts were made to measure the relative intensities of emission lines in the furnace spectrum of iron, but self-reversal by the cooler vapors at the ends of the tube was found to be strong in the case of low-level lines. Since it seemed to be impossible to eliminate this self-reversal or to correct for it satisfactorily, it was decided to attempt intensity measurements on iron lines in absorption. Before describing the method used, it will be necessary to consider briefly the processes involved in the formation of an absorption line in a heated vapor by the absorption of light from the continuous spectrum of a hot source. That is, we must describe the curve of growth of an absorption line.

By the curve of growth is meant the functional relation between the total absorption of a line and the number of atoms active in absorbing the line.

The total absorption of a spectral line has been defined[6] as

$$A = \frac{I}{I_0},$$

[4] R. Frerichs, *Ann. d. Phys.*, **81**, 807, 1926; J. B. van Milaan, *Zs. f. Phys.*, **38**, 427, 1926; G. R. Harrison, *J. Opt. Soc. Amer.*, **17**, 389, 1928.

[5] G. R. Harrison, *J. Opt. Soc. Amer.*, **19**, 109, 1929; R. S. Seward, *Phys. Rev.*, **37**, 344, 1931.

[6] R. Ladenburg and F. Reiche, *Ann. d. Phys.*, **42**, 181, 1913.

where I and I_0 are, respectively, the absorbed energy and the incident energy. Since

$$I=I_0\int_{-\infty}^{+\infty}(1-e^{-k\nu l})d\nu \ ,$$

where $k\nu$ is the absorption coefficient and l the length of the column of absorbing vapor,

$$A=\int_{-\infty}^{+\infty}(1-e^{-k\nu l})d\nu \ .$$

When the general equation for the absorption coefficient, providing for combined Doppler effect and natural broadening, is substituted for $k\nu$ and the equation integrated for various values of the parameter a, the natural damping ratio, appearing in the expression for the absorption coefficient, A may be derived as a function of the number of atoms active in absorbing the line. This integration has been carried out graphically by Schütz[7] and by Van der Held.[8] More specifically, log (const. $\times A/b$) is derived as a function of log (Nfl/b). The quantity b is the Doppler breadth, depending only on the absolute temperature T, the molecular weight M, and the central frequency ν_0:

$$b=\text{const. } \nu_0\sqrt{\frac{T}{M}} \ .$$

N is the number of atoms per cubic centimeter and l the length of the absorbing column; f, the so-called "oscillator strength" of the line, is the factor by which the energy absorbed per unit time by the classical oscillator must be multiplied to give the energy absorbed per unit time by the same number of atoms. In the classical dispersion theory the quantity $\boldsymbol{N}=Nf$, the "number of dispersion electrons," appears. In the quantum theory f is proportional to the Einstein A coefficient, or, in the case of resonance lines, inversely proportional to the lifetime of the resonance level.

Van der Held[8] gives numerical values for (const. $\times A/b$) as a function of log (Nfl/b) for four values of the natural damping ratio a.

[7] *Zs. f. Ap.*, **1**, 300, 1930. [8] *Zs. f. Phys.*, **70**, 508, 1931.

From these the total absorptions or equivalent widths for any element at any temperature and wave-length can be plotted as a function of log (Nfl/b) and the curves of growth constructed for the various values of a. This has been done by the writers for iron at a temperature of 2100° C and wave-length λ 4000 A. The resulting curves are shown in Figure 1.

For very faint lines, below about 0.03 A EW, the Doppler effect due to thermal motion of the atoms allows each absorbing atom to contribute its full absorbing power to the absorption coefficient, and

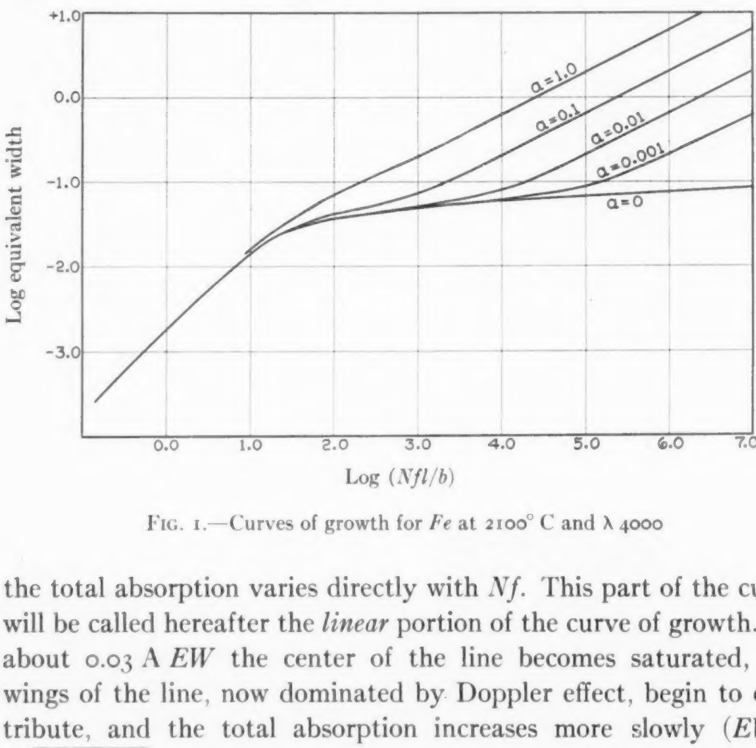

FIG. 1.—Curves of growth for Fe at 2100° C and λ 4000

the total absorption varies directly with Nf. This part of the curve will be called hereafter the *linear* portion of the curve of growth. At about 0.03 A EW the center of the line becomes saturated, the wings of the line, now dominated by Doppler effect, begin to contribute, and the total absorption increases more slowly ($EW \propto \sqrt{\log Nf+C}$). Finally, for high concentrations the natural damping operating in the wings of the line begins to take hold, at a point depending on the size of a, and the $EW \propto \sqrt{Nf}$. The different slopes for the Doppler and the natural damping portions of the curve are due to the fact that the Doppler structure of the line falls off exponentially at the edges of the line, while the natural structure de-

creases quadratically. The Doppler and the radiation-damping portions of the curve may be influenced by external effects such as collisions or Stark effect, but the slope of the linear portion is not subject to these effects, since it is obviously impossible for the total absorption to increase more rapidly than Nf. Hence, in studying the linear part, higher pressures may be used than are possible for the Doppler or the damping portions.

Many years before the development of the theory, the whole course of the curve of growth was observed by Gouy[9] by measuring the relative intensities of the sodium D lines for different concentrations of sodium in a flame. Since the development of the theory, there has been ample verification by many investigators, also mainly based on measures of the intensities of resonance doublets at known concentrations. Notably, the Doppler and the damping portions have been investigated by Schütz;[10] the linear, Doppler, and damping portions by Ornstein and Van der Held;[11] and recently Minkowski, Müller, and Weber-Schäfer[12] have used the linear portion in measuring the transition probabilities for the sodium D lines. Curves of growth have been computed by Minnaert and Slob[13] for a Fraunhofer line with a Pannekoek profile, and the whole curve of growth from the linear region to the damping region has been traced with lines in the solar spectrum by means of values of Nf derived from the Adams-Russell calibration of the Rowland scale.[14]

It should be possible, therefore, to use either the linear or the damping portions of the curve of growth for measurements of the relative intensities of lines in complex spectra, provided the portion of the curve used can be obtained free from distortion under our laboratory conditions. In this work the linear portion of the curve—the region of very faint lines—has been used, for reasons which are discussed later.

The relations between the various expressions for line intensity

[9] *Ann. Chim. Phys.*, **18** (5), 5, 1879.

[10] *Zs. f. Ap.*, **1**, 300, 1930.

[11] *Zs. f. Phys.*, **77**, 469, 1932.

[12] *Zs. f. Phys.*, **94**, 145, 1935.

[13] *Proc. Acad. Amsterdam*, **34**, 542, 1931.

[14] Minnaert and Mulders, *Zs. f. Ap.*, **2**, 165, 1931.

used in experimental and theoretical work for lines differing considerably in wave-length may be stated as follows:

$$\frac{f}{\nu} \propto \frac{A}{\nu^3} \propto \frac{I}{\nu^4} \propto |a|^2 ,$$

where ν is the frequency of the line, f the f-value, A the Einstein coefficient of spontaneous emission, I the emission intensity of the line, and $|a|^2$ the sum of the squares of the matrix elements between the two states in question. The latter quantity is proportional to the multiplet intensity numbers first derived from the correspondence principle and subsequently by the quantum mechanics. Hence, if the quantities measured are f-values for lines differing widely in wave-lengths, they must be multiplied by ν^3 to be comparable with emission intensities, or divided by ν to compare them with the theoretical multiplet intensity numbers.

The *equivalent width* of an absorption line is defined as the fraction of a strip of the neighboring continuous spectrum 1 A wide absorbed by the line. On the linear portion of the curve of growth the total absorption A in a frequency interval $d\nu$ is proportional to f:

$$A d\nu \propto f ,$$

whence

$$A \frac{d\lambda}{\lambda^2} \propto f .$$

Hence, if $d\lambda$ is measured in angstroms, the quantity $A d\lambda$ is the equivalent width. Therefore, if the unit of measurement is equivalent width, the relative intensities derived from the curve of growth for lines of widely different λ must be divided by λ^2 to correspond to relative f-values (these must also, of course, be reduced to infinite temperature).

FURNACE SPECTRA AND PHOTOMETRY

In the experiments a 50-amp. Philips cinema lamp with a tungsten coil filament in a quartz bulb, operated at about 3100° C, was used as the source of the continuous spectrum. The light, rendered parallel by a lens of 8-cm focus, was passed through the furnace tube and

focused on the slit of the 15-foot concave-grating spectograph. The cylindrical furnace,[15] constructed primarily for use at high pressures, was used in preference to the newer hood furnace[16] because a lower pressure could be maintained and experiments could be made with tubes of different lengths up to 40 cm. The maintenance of a constant temperature in this furnace was more difficult, however, on account of occasional variations in the contact between the tube and the bronze clamps. Although the furnace was not free from leaks, pressures of 0.5 mm of *Hg* or less were easily maintained. The second order of the 15-foot concave-grating spectrograph (dispersion = 1.86 A/mm) was used throughout.

The measurement of the total absorption of the very faint lines appearing on the linear portion of the curve of growth necessitated the use of high-contrast, fine-grained plates. An emulsion equivalent to the Eastman IV type seems most satisfactory. Eastman contrast Bromide and IV-O plates were used in the wave-length region $\lambda\lambda$ 3650–4400 so far studied. Exposure times were in the neighborhood of 2 minutes.

To obtain plate calibration-curves, the spectrograph slit was replaced by a step-slit; and density strips were impressed on the plates with the aid of a tungsten ribbon filament lamp. The step-slit has nine openings, the widths of which are approximately in the ratio 1:1.5. Since the astigmatism of the concave grating requires that each opening be exposed separately, the step-slit was constructed so that each opening could be placed separately in the center of the optical system. Separate exposures necessitated great care in keeping the lamp current constant and the exposure times equal. The exposure time for each opening was equal to that for the furnace absorption spectra to be calibrated.

The spectrograph plateholder takes a plate $1\frac{3}{4}\times 18$ inches. A plate $3\frac{1}{2}\times 18$ inches was cut into two strips, on one of which were recorded the furnace absorption spectra, usually three or four, and on the other the calibration strips. Both halves of the plate were developed together for 4 minutes in X-ray developer at a temperature

[15] A. S. King, *Mt. W. Contr.*, No. 28; *Ap. J.*, **28**, 300, 1908.

[16] A. S. King, *Mt. W. Contr.*, No. 247; *Ap. J.*, **56**, 318, 1922.

of 18° C. Plates were brushed during development to minimize the Eberhard effect.

Tracings of all the spectra were made with the photoelectric recording microphotometer designed (and constructed) by Dunham. The highest magnification available, 1 : 100, was used for the absorption lines.

Characteristic curves at wave-length intervals of 100 A were constructed for each plate. The equivalent widths of the absorption lines were derived with the aid of these curves. The density profiles recorded by the microphotometer were converted into intensity profiles by a short method, and the areas under the intensity profiles then reduced to equivalent widths in angstrom units.

MEASUREMENT OF RELATIVE f-VALUES

Two different parts of the curve of growth might be used to derive the relative f-values from the measured equivalent widths of lines appearing in absorption spectra—the linear portion where $EW \propto Nf$, and the natural damping portion where $EW \propto \sqrt{Nf}$. It should be made clear that, unless N, l, and b are all known, only the relative f-values are measurable. The quantity b depends only on the wave-length, temperature, and atomic weight and can be calculated; l, the length of the furnace tube, is known; but N, the number of atoms per cubic centimeter, cannot be found with any degree of certainty without accurate knowledge of the vapor pressure. This seems impossible with the present apparatus because, for one reason, with the high temperatures needed no transparent substance can be used for windows to close the tube at the ends of the heated portion.

Since the radiation-damping portion of the curve is very sensitive to external influence, such as collision broadening, its observation requires very low pressures and a long column of vapor. With the length of tube available, no iron lines reached the damping portion of the curve at the pressures used (0.1–0.5 mm of Hg), which were much too high to avoid collision broadening on the damping portion, although low enough to avoid its effects on the Doppler portion. The slopes of the linear portion and, at moderately low pressures, of the Doppler portion are not influenced by external effects. The linear portion of the curve of growth has therefore been used for the

measurement of the relative f-values. The main objection to using this portion is the faintness of the lines and the consequent uncertainty in measuring their equivalent widths. This disadvantage is partially compensated by the fact that $EW \propto Nf$, which enables a more precise determination of f than in the damping region where $EW \propto \sqrt{Nf}$. The large uncertainty in the measurements of equivalent widths requires many measures on each line.

Since N, l, and b are constant for all the lines appearing on any one spectrogram, the equivalent widths of the faint lines appearing in the linear region will be directly proportional to their relative f-values at that temperature. Essentially the procedure followed in deriving relative f-values has been to hold b and l constant and to vary N. Beginning with a very small charge of iron (small N) in the furnace and gradually increasing it, measurements are made of the equivalent widths of lines which appear on the linear portion of the curve of growth for each of the successive charges. Finally, a saturated condition is reached when an increased charge no longer increases N unless the pressure or temperature is also increased. Although the absolute value of N at any stage is unknown, two spectra for which N is slightly different have enough lines in common in the linear region to permit a reduction of the relative f-values of all the lines in the two spectra to the same scale. By extending this process the relative f-values derived from the whole series of spectra for all values of N can be reduced to this scale. A range in f-values of about 3500 to 1 has thus been covered at one temperature, although the range for lines appearing in the usable part of the linear portion of the curve for one value of N is only about 16 to 1. The relative f-values thus determined for lines arising from different levels must be reduced to infinite temperature by means of the Boltzmann formula. Suitable wave-length corrections already described must also be applied to make the results proportional to transition probabilities, to emission intensities, or to theoretical multiplet intensities.

A furnace temperature of 2100° C was used in the work reported here. At higher temperatures the measurements may, of course, be extended to multiplets of higher excitation potential.

At the pressures used, the influence of collision broadening on the Doppler portion of the curve of growth should be negligible. The

lower part of the Doppler region, just above the linear portion, was not appreciably affected by pressures of several millimeters of *Hg*.

OBSERVATIONAL TEST OF THE METHOD

Before the linear part of the theoretical curve of growth can be used for the derivation of relative *f*-values from the measured equivalent widths of faint absorption lines, it must be shown that this part of the curve gives valid results under the experimental conditions used. This can be done by measuring the equivalent widths of a group of lines in the linear part of the curve whose relative intensities over a wide range are known from experiment. Probably the most suitable data for this purpose are Harrison's measures of the relative intensities of lines in multiplets of *Ti* I made with high precision in the arc spectrum.[17]

Spectrograms were taken with titanium in the furnace, and the equivalent widths of the lines in four multiplets of *Ti* I at 2000° C and in one at 2100° C were measured. These multiplets were $a^3F-y^3G^o$, $a^3F-x^3F^o$, $a^3F-y^3D^o$, $a^3F-y^3F^o$, all arising from the normal state, and $a^5F-x^5D^o$ with a low *EP* of about 0.8 volt. Each multiplet was measured several times on spectra with slightly different values of N. The observed equivalent widths were plotted against Harrison's intensities; the resulting curves drawn through the points were then compared with the theoretical curve of growth for the mean λ for each multiplet by shifting the observed curves horizontally until they coincided with the theoretical curves. Finally, all the observed and theoretical curves were superposed. The result is shown in Figure 2. Each point is an individual measure of the equivalent width of one line on one plate. The curve is the theoretical curve of growth for *Ti* at 2000° C and λ 3660. While the scatter in the points is somewhat large, there are no significant deviations from the theoretical curve.

The agreement is illustrated more clearly, perhaps, by comparing the relative intensities for the lines of these *Ti* multiplets derived from the theoretical curve of growth with Harrison's relative arc intensities. Figure 3 shows the results. Here each point represents the mean of several measures of the intensities derived from the

[17] G. R. Harrison, *J. Opt. Soc. Amer.*, 17, 389, 1928.

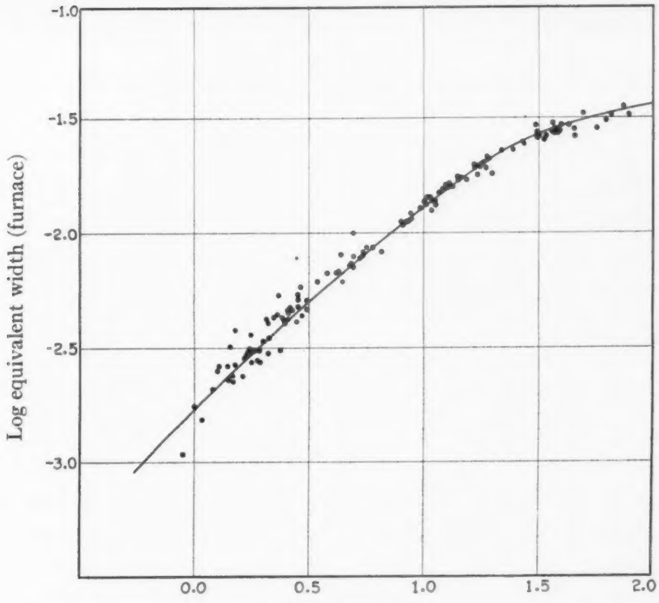

FIG. 2.—Comparison of equivalent widths of furnace absorption lines in multiplets of *Ti* I with Harrison's arc intensities.

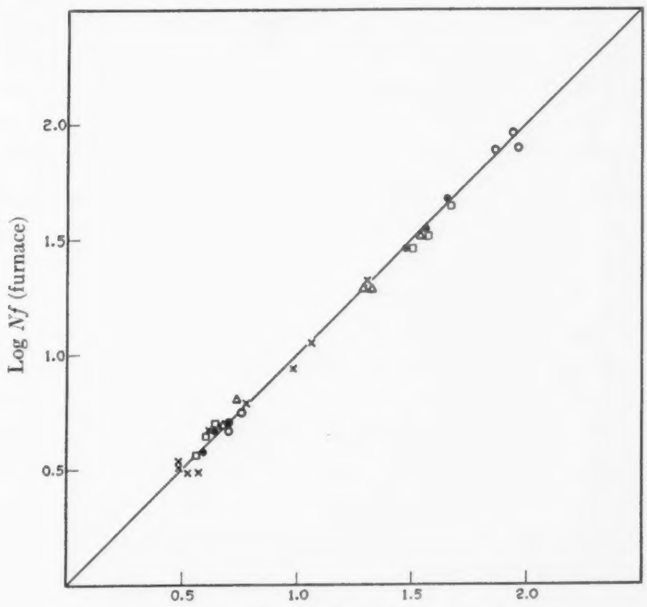

FIG. 3.—Comparison of intensities derived from linear part of the curve of growth with Harrison's arc intensities for lines in multiplets of *Ti* I.

equivalent widths for each line of the five multiplets. The straight lines drawn through the points representing the lines of each multiplet have been superposed. The lines of different multiplets are distinguished by different symbols. Harrison's intensity values have been corrected for the Boltzmann distribution within the multiplets at the temperature used. These corrections were also applied to Harrison's intensities used in Figure 2, but no wave-length corrections were applied. It is seen that the points in Figure 3 lie scattered along a 45° line, thus indicating an absence of systematic errors in the linear part of the theoretical curve of growth from which the observed intensities have been derived. The use of the linear part of the theoretical curve of growth to derive relative *f*-values for iron lines from their observed equivalent widths seems therefore to be justified. Scattered light and other possible influences apparently do not appreciably distort this part of the curve.

BOLTZMANN DISTRIBUTION IN THE ELECTRIC FURNACE

Since the primary advantage in this method of intensity measurement rests in the condition of thermal equilibrium supposed to exist in the furnace, it is important to verify this condition by experiment. It must be shown that the distribution of atoms in the low levels is in accordance with the Boltzmann distribution law at that temperature.

This condition was assumed for the lines of *Ti* treated in the preceding section, and temperature corrections were applied to Harrison's arc intensities; but the wave-number differences between low levels within the *Ti* multiplets used is too small to furnish a check on the validity of the assumption.

The Boltzmann formula provides that, if the atoms are in thermal equilibrium, the relative numbers of atoms in two states, 1 and 2, are given by:

$$\frac{N_1}{N_2}=\frac{g_1 e^{-E_1/KT}}{g_2 e^{-E_2/KT}},$$

where g_1 and g_2 are the statistical weights of the states, E_1 and E_2 the energies, K the Boltzmann constant, and T the absolute temperature. Hence, to correspond to the a priori transition probabilities,

the intensities of lines arising from levels above the normal level at a given temperature must be multiplied by a factor:

$$R=\frac{e^{-E_1/KT}}{e^{-E_2/KT}}=e^{\frac{hc}{KT}\Delta\nu} ,$$

where $\Delta\nu$ is the wave-number difference from the normal state. In practice this may be used in the more convenient form[18]

$$\log R=\frac{0.625\Delta\nu}{T} .$$

At temperatures in the neighborhood of 2100° C the weaker lines of the *Fe* multiplets $a^5D-z^5F^\circ$ and $a^5D-z^5D^\circ$ arising from the normal level are of the same order of intensity as the stronger lines of the multiplets $a^5F-y^5F^\circ$ and $a^5F-y^5D^\circ$ arising from a level about 7000 wave numbers above the normal level; that is, several lines arising from each level appear on the linear part of the curve of growth at the same time. A spectrogram was taken with the furnace at a temperature of 2400° C with a very small charge of iron in the furnace, so that these lines were in the linear part of the curve of growth for that temperature. Another spectrogram was taken at 1800° C with a larger charge of iron, so that the same lines were again in the linear portion of the curve. The relative intensities were derived from the curve of growth for each temperature. Values of R computed for each line at both temperatures were multiplied by the measured intensities. If the atoms in the furnace are in a condition of thermal equilibrium, the increase in the intensity of the lines arising from the a^5F level relative to those arising from the a^5D level when the temperature is raised from 1800° C to 2400° C should be accounted for by the Boltzmann formula. This is found to be the case within the limits of experimental error, as shown by the results in Table I. The lines arising from the a^5D term are listed in the upper half of the table and those from a^5F in the lower half. The first three columns give the wave-length, the multiplet designation, and the low term value in cm^{-1}. The next three columns give the value of R, the measured relative intensities (on an arbitrary scale), and the product RNf for 1800° C. The next three columns give the cor-

[18] G. R. Harrison, *J. Opt. Soc. Amer.*, **19**, 109, 1929.

responding values for 2400° C. The ratio of RNf at 1800° C to RNf at 2400° C is in the last column. Physically, this ratio is the ratio of N, the number of atoms per cubic centimeter in the furnace, for the two spectra, and should be constant for all lines. The mean values of this ratio for the lines arising from the low a^5D term and from the higher a^5F term are 1.74 ± 0.11 and 1.82 ± 0.17, respectively. Since

TABLE I

TEST OF BOLTZMANN FORMULA

λ	Multiplet	$\Delta\nu$	1800° C			2400° C			$\frac{RNf(1800°C)}{RNf(2400°C)}$
			R	Nf	RNf	R	Nf	RNf	
3733.32..	$a^5D_1-z^5F_1^\circ$	888.1	1.85	16.2	30.9	1.61	11.2	18.0	1.72
3745.90..	$a^5D_0-z^5F_1^\circ$	978.1	1.97	17.8	34.9	1.69	11.5	19.4	1.80
3824.44..	$a^5D_4-z^5D_3^\circ$	0.0	1.00	29.5	29.5	1.00	15.2	15.2	1.94
3856.37..	$a^5D_3-z^5D_2^\circ$	415.9	1.425	25.1	35.8	1.25	14.6	18.2	1.96
3878.58..	$a^5D_2-z^5D_1^\circ$	704.0	1.625	17.9	29.1	1.46	11.2	16.3	1.78
3899.71..	$a^5D_2-z^5D_2^\circ$	704.0	1.625	15.5	25.2	1.46	9.48	13.9	1.81
3906.48..	$a^5D_1-z^5D_1^\circ$	888.1	1.85	3.12	5.78	1.61	2.33	3.75	1.54
3920.26..	$a^5D_0-z^5D_1^\circ$	978.1	1.97	9.37	5.95	1.69	18.5	10.1	1.83
3922.91..	$a^5D_3-z^5D_4^\circ$	415.9	1.425	14.0	20.0	1.25	9.65	12.1	1.65
3927.92..	$a^5D_1-z^5D_2^\circ$	888.1	1.85	12.9	23.9	1.61	9.22	14.8	1.62
3930.30..	$a^5D_2-z^5D_3^\circ$	704.0	1.625	16.4	26.7	1.46	11.5	16.8	1.60
Mean.	....	......	......	......	......	......	......	......	1.74 ± 0.11
3734.87..	$a^5F_5-y^5F_5^\circ$	6928.3	122.6	11.5	1410	41.6	17.5	729	1.93
3749.49..	$a^5F_4-y^5F_4^\circ$	7376.8	167	6.44	1110	53.0	10.5	556	1.99
3758.24..	$a^5F_3-y^5F_3^\circ$	7728.1	212	3.43	728	63.6	7.28	463	1.57
3763.79..	$a^5F_2-y^5F_2^\circ$	7985.8	255	2.11	538	73.0	3.93	287	1.86
3767.19..	$a^5F_1-y^5F_1^\circ$	8154.7	289	1.19	344	80.4	2.66	214	1.61
3820.43..	$a^5F_5-y^5D_4^\circ$	6928.3	122.6	8.70	1070	41.6	13.2	550	1.95
3825.88..	$a^5F_4-y^5D_3^\circ$	7376.8	167	4.96	828	53.0	7.59	402	2.05
3834.23..	$a^5F_3-y^5D_2^\circ$	7728.1	212	1.85	392	63.6	3.79	241	1.62
Mean.	....	......	......	......	......	......	......	......	1.82 ± 0.17

the agreement is within the errors of measurement, we are justified in considering the atoms in the furnace to be in a condition of thermal equilibrium.

RESULTS

The relative intensities at 2100° C of the lines in nine multiplets of iron in the region λλ 3650–4325 have been measured. Two multiplets of temperature class I, $a^5D - z^5F^\circ$ and $a^5D - z^5D^\circ$, arise from the normal level, as does the intersystem multiplet $a^5D - z^7P^\circ$ (class

I A). Three multiplets of class II, $a^5F-y^5F^o$, $a^5F-z^3P^o$, and $a^5F-y^5D^o$, arise from the next low term, a^5F ($EP=1.0$ volt). Three multiplets of class II, $a^3F-y^3D^o$, $a^3F-y^3F^o$, and $a^3F-z^3G^o$, arise from the next term above the a^5F level, a^3F ($EP=1.5$ volts). The sublevels of the three low terms, their distance in wave numbers above the ground term, and their corresponding values of R for a temperature of 2100° C are given in Table II. The large values of R for the a^3F term are notable.

TABLE II

BOLTZMANN FACTORS FOR LOW TERMS OF *Fe* I AT 2100° C

Term	$\Delta\nu$	R	Term	$\Delta\nu$	R	Term	$\Delta\nu$	R
a^5D_4....	0.0	1.00	a^5F_5 ...	6928.3	66.0	a^3F_4....	11976.3	1396
a^5D_3....	415.9	1.29	a^5F_4....	7376.8	86.5	a^3F_3....	12560.9	1989
a^5D_2....	704.0	1.53	a^5F_3....	7728.1	107.0	a^3F_2....	12968.6	2545
a^5D_1....	888.1	1.71	a^5F_2....	7985.8	125.1			
a^5D_0....	978.1	1.81	a^5F_1....	8154.7	138.5			

Relative intensities at 2100° C were derived from the measured equivalent widths by means of the linear portion of the curve of growth computed for *Fe* at 2100° C and λ 4000. Only the upper portion of the linear part of the curve between values of log *EW* of about -2.5 to -1.6 was used (Fig. 1).

To adjust the relative intensities to the same scale the plates were divided into two groups—one for which N was small and on which only the class I lines and stronger class II lines appeared in the linear region, and one for which N was large and on which the weaker class II and the I A lines appeared. The relative intensities obtained from the plates of each group were adjusted to the scale of a plate from the middle of the group for which the temperature was known to be constant and combined into mean values. Since these two groups had few lines in common, a special plate was obtained for which N was between the values for the two groups, and which contained numerous lines in common with both groups. Good factors were thus obtained by which the lines of the strong and weak groups were reduced to the same scale. The zero point of the scale is, of course, an arbitrary one, owing to the fact that the absolute value of N is unknown.

TABLE III

RELATIVE *f*-VALUES FOR LINES OF *Fe* I

λ	Multiplet	Int. (2100° C)	$f=R\cdot$Int.	No. Meas.
3649.51	$a^5D_4-z^5F^\circ_3$	2.7*	2.7*	5
3679.92	$a^5D_4-z^5F^\circ_4$	61	61	16
3683.05	$a^5D_3-z^5F^\circ_2$	7.0	9.0	9
3705.57	$a^5D_3-z^5F^\circ_3$	82	110	13
3707.83	$a^5D_2-z^5F^\circ_1$	8.5	13	9
3719.94	$a^5D_4-z^5F^\circ_5$	530 *	530 *	7
3722.56	$a^5D_2-z^5F^\circ_2$	77	120	13
3733.32	$a^5D_1-z^5F^\circ_1$	54	92	14
3737.13	$a^5D_3-z^5F^\circ_4$	350 *	450 *	8
3745.56	$a^5D_2-z^5F^\circ_3$	220	340	8
3745.90	$a^5D_0-z^5F^\circ_1$	61	110	16
3748.26	$a^5D_1-z^5F^\circ_2$	110	190	11
3824.44	$a^5D_4-z^5D^\circ_3$	87	87	12
3856.37	$a^5D_3-z^5D^\circ_2$	84	110	12
3859.91	$a^5D_4-z^5D^\circ_4$	350	350	6
3878.56	$a^5D_2-z^5D^\circ_1$	58	88	12
3886.28	$a^5D_3-z^5D^\circ_3$	130	160	10
3895.66	$a^5D_1-z^5D^\circ_0$	30	52	13
3899.71	$a^5D_2-z^5D^\circ_2$	46	70	13
3906.48	$a^5D_1-z^5D^\circ_1$	11	19	10
3920.26	$a^5D_0-z^5D^\circ_1$	26	48	13
3922.91	$a^5D_3-z^5D^\circ_4$	45	58	15
3927.92	$a^5D_1-z^5D^\circ_2$	41	70	16
3930.30	$a^5D_2-z^5D^\circ_3$	51	78	16
4206.70	$a^5D_3-z^7P^\circ_3$	0.47	0.60	4
4216.19	$a^5D_4-z^7P^\circ_4$	2.1	2.1	5
4258.32	$a^5D_2-z^7P^\circ_3$	0.23*	0.36*	3
4291.47	$a^5D_3-z^7P^\circ_4$	0.33	0.42	5
3687.46	$a^5F_5-y^5F^\circ_4$	6.5	430	7
3709.25	$a^5F_4-y^5F^\circ_3$	8.1	710	10
3727.62	$a^5F_3-y^5F^\circ_2$	7.1	760	9
3734.87	$a^5F_5-y^5F^\circ_5$	72	4700	12
3743.34	$a^5F_2-y^5F^\circ_1$	4.5	560	8
3749.49	$a^5F_4-y^5F^\circ_4$	43	3700	13
3758.24	$a^5F_3-y^5F^\circ_3$	26	2800	13
3763.79	$a^5F_2-y^5F^\circ_2$	14	1800	11
3767.19	$a^5F_1-y^5F^\circ_1$	9.1	1300	10
3787.88	$a^5F_1-y^5F^\circ_2$	3.6	500	4
3795.00	$a^5F_2-y^5F^\circ_3$	4.7	590	7
3798.51	$a^5F_4-y^5F^\circ_5$	2.9	260	5
3799.55	$a^5F_3-y^5F^\circ_4$	4.6	500	6
3786.68	$a^5F_1-z^3P^\circ_0$	0.27*	37*	7
3790.10	$a^5F_2-z^3P^\circ_1$	0.75	94	7
3812.97	$a^5F_3-z^3P^\circ_2$	3.1	330	8
3814.53	$a^5F_1-z^3P^\circ_1$	0.17*	24*	8
3850.82	$a^5F_2-z^3P^\circ_2$	0.81	100	8

TABLE III—*Continued*

λ	Multiplet	Int. (2100° C)	$f=R\cdot$Int.	No. Meas.
3820.43	$a^5F_5-y^5D^\circ_4$	47	3100	16
3825.88	$a^5F_4-y^5D^\circ_3$	26	2200	16
3834.23	$a^5F_3-y^5D^\circ_2$	14	1500	11
3840.44	$a^5F_2-y^5D^\circ_1$	7.0	870	11
3849.97	$a^5F_1-y^5D^\circ_0$	3.7	510	9
3865.53	$a^5F_1-y^5D^\circ_1$	3.0	420	9
3872.50	$a^5F_2-y^5D^\circ_2$	3.3	410	11
3878.02	$a^5F_3-y^5D^\circ_3$	3.9	420	11
3887.05	$a^5F_4-y^5D^\circ_4$	3.1	270	10
3898.01	$a^5F_1-y^5D^\circ_2$	0.38	53	5
3917.19	$a^5F_2-y^5D^\circ_3$	0.34	42	4
3940.88	$a^5F_3-y^5D^\circ_4$	0.15*	16*	5
3815.84	$a^3F_4-y^3D^\circ_3$	3.7	5200	8
3827.83	$a^3F_3-y^3D^\circ_2$	2.4	4700	8
3841.05	$a^3F_2-y^3D^\circ_1$	1.4	3600	8
3888.52	$a^3F_2-y^3D^\circ_2$	0.49	1200	7
3902.95	$a^3F_3-y^3D^\circ_3$	0.91	1800	8
3969.26	$a^3F_4-y^3F^\circ_3$	1.1	1500	8
4005.25	$a^3F_3-y^3F^\circ_2$	0.60	1200	8
4045.82	$a^3F_4-y^3F^\circ_4$	4.0	5500	6
4063.60	$a^3F_3-y^3F^\circ_3$	2.3	4500	8
4071.75	$a^3F_2-y^3F^\circ_2$	1.5	3900	8
4132.06	$a^3F_2-y^3F^\circ_3$	0.41	1100	6
4143.87	$a^3F_3-y^3F^\circ_4$	0.71	1400	8
4202.03	$a^3F_4-z^3G^\circ_4$	0.66	920	8
4250.79	$a^3F_3-z^3G^\circ_3$	0.46	920	7
4271.76	$a^3F_4-z^3G^\circ_5$	1.7	2400	8
4307.91	$a^3F_3-z^3G^\circ_4$	1.6	3200	8
4325.77	$a^3F_2-z^3G^\circ_3$	1.5	3800	8

The results are given in Table III. The third column shows the measured relative intensities at 2100° C multiplied by the value of R corresponding to the low-term value taken from Table II and divided by λ^2, all adjusted to the same scale as described in the preceding paragraph. The fourth column contains the products $R\cdot$Int. (2100° C). These quantities are proportional to the real f-values for the lines, but on an arbitrary scale. Owing to scarcity of measures on the strongest and the weakest lines, values for these lines are the most uncertain and are marked with an asterisk. Each of the measures noted in the last column was made on a different spectrogram. The average deviations of the individual intensity measures from the mean values vary from 4 to 15 per cent for different lines. The average mean deviation is about 8 per cent.

SOURCES OF ERROR

The sources of error may be divided roughly into two classes: (1) errors of photographic photometry common to any absorption-line intensity work, which, however, show themselves mainly as random accidental errors when many independent measures are made; (2) errors peculiar to the method, which may affect the results systematically but which have not yet shown themselves.

Errors of the first kind include uneven development, plate grain, errors in the calibration-curves, errors in microphotometry such as uncertainty in the clear glass reading, and others, most of which are small in comparison with the general uncertainty in measuring the total absorption of very faint lines. It is quite obvious that this method cannot hope to equal the precision possible in the best emission spectra methods. The only recourse is numerous independent repetitions of the measures on each line in order to cut down the uncertainty as much as possible. Another photometric source of error, which may not be random, lies in the drawing-in of the continuous background. Professor R. Minkowski has found[19] that there is a tendency to make the continuous background too faint. This would tend to make the equivalent widths too small and would have a larger percentage effect on faint lines than on strong lines.

Errors of the second kind are more serious. The good agreement of the linear part of the theoretical curve of growth with Harrison's intensities for titanium does not exclude the possibility of a slight systematic difference between the observed curve of growth under the conditions used and the theoretical curve. Although there is no reason to suspect it, a slight deviation from thermal equilibrium would seriously affect the factor R and thus introduce large errors. Small variations in temperature during the exposure, which are known to have occurred, may also have introduced systematic errors, although it is probable that they appear in the results mainly as random errors, increasing the value of the probable error. Temperature variations, however, can be completely eliminated in future work. Another source of error, akin to self-reversal in emission spectra but working in the opposite direction, is the absorption by the small layer of cooler vapor at the ends of the open furnace tube. The

[19] Verbal communication.

effect of this layer should be to increase the absorption of the lowest-level lines relative to higher-level lines, since a larger proportion of the atoms in this cooler layer will be in the normal state than in the upper states. The good check obtained on the Boltzmann formula seems, however, to indicate that this effect is small.

In conclusion, it may be pointed out that the measurement of the total absorption, at a known concentration of atoms, of one of the lines for which we have given relative f-values would put the whole series of results on an absolute scale. This would, of course, greatly enhance their value for astrophysical purposes.

The measurements of relative f-values for lines of *Fe* I are being extended to lines of longer wave-length and higher temperature classes.

We wish to express our thanks to Professors H. N. Russell and Rudolph Minkowski for very valuable advice and discussion, and especially to Dr. Theodore Dunham, Jr., for many helpful suggestions throughout the course of the work.

CARNEGIE INSTITUTION OF WASHINGTON
MOUNT WILSON OBSERVATORY
August 1935

THE GLOBULAR CLUSTER NGC 2419*

By W. BAADE

ABSTRACT

Owing to its unusually large distance and its position in the anticenter region of our galaxy, the globular cluster NGC 2419 is of exceptional interest. The discovery in the cluster of 36 variable stars, 31 of which are short-period Cepheids, made it possible to obtain a reliable determination of the distance modulus. The result is $m-M=19.24\pm 0.01$, which agrees closely with the value 19.17 derived from the 25 brightest cluster-stars. Counts of nebulae in the surrounding field and the absence of selective absorption in the light of NGC 2419 indicate that the field of the cluster is free from local obscuration. The photometric distance must, however, be corrected for the general absorption within our galaxy (latitude effect), which reduces the measured modulus from 19.22 to 18.75 mag., corresponding to a distance of 56,000 parsecs. The question whether NGC 2419 is a member of our galaxy or an independent system is discussed.

INTRODUCTION

NGC 2419 was discovered by W. Herschel, who described it as cB, R, vGmbM, about 3′d. Although reobserved by Lord Rosse,[1] Schultz, Schoenfeld, Bigourdan, and probably by others, its true nature was recognized only thirteen years ago by C. O. Lampland on plates taken at the Lowell Observatory.[2] Lampland's observations made it at once apparent that NGC 2419 is a globular cluster of uncommon interest. Its distance must be very large, even for a globular cluster, because of the unusual faintness of the stars and its small angular diameter. The great distance thus suggested is the more surprising since its position in the sky is nearly opposite that of the galactic center, i.e., in a region where we should expect only nearby globular clusters, if any at all. The first estimate of the distance of NGC 2419 was given by H. Shapley, who, from the apparent diameter, found a value of 50,000 parsecs.[2] Later, in his *Star Clusters*, he

* *Contributions from the Mount Wilson Observatory, Carnegie Institution of Washington*, No. 529.

[1] The notes of the Birr Castle observers contain the first hints that NGC 2419 might be a globular cluster (*Scientific Trans. R. Dublin Soc.*, Ser. II, **2**, 60, 1878). It seems that even the brightest stars of NGC 2419 could not be seen with certainty with the large 6-foot reflector and that the surmise was based upon the general appearance of the object. Dreyer in his NGC description made no reference to the conjectures of the Birr Castle observers.

[2] *H.B.*, No. 776, 1922.

published the revised value 30,000 parsecs, corresponding to the modulus $m-M=17.4$, which he derived from the angular diameter and the total apparent brightness of the cluster. Obviously, both determinations are of low weight. Since the appearance of the cluster on plates taken with the Mount Wilson reflectors could not be reconciled with a modulus as small as 17.4 and indicated one somewhat fainter than magnitude 19, it seemed desirable to determine the distance by more reliable methods.

VARIABLE STARS IN NGC 2419

Short-period Cepheids, if they can be found, offer the best possibility of obtaining an accurate value for the distance of a globular cluster. The search for such variables in NGC 2419 confirmed the unusual faintness of the cluster stars, since under average seeing conditions 1-hour exposures with the 100-inch reflector were necessary

TABLE I

RECTANGULAR CO-ORDINATES OF VARIABLE STARS IN NGC 2419

No.	x	y	No.	x	y
1	+ 40″	− 52″	21	− 55″	+ 30″
2	− 4	− 19	22	+109	− 5
3	+ 52	− 24	23‡	+ 27	+ 79
4	+ 80	− 15	24	−147	− 10
5*	+ 33	+ 47	25	− 59	+ 38
6	+ 56	−127	26§	− 70	− 50
7	+ 91	+ 87	27	+ 19	−103
8	− 17	+ 41	28	−192	+ 59
9	− 32	+ 88	29	− 58	− 7
10	+ 20	− 51	30	− 26	+ 23
11	+ 95	− 8	31	+154	−146
12	+133	+111	32	− 19	+ 48
13	+101	− 10	33	+ 47	− 17
14	−115	− 13	34	+ 21	+157
15	+ 62	+ 40	35	+ 43	+ 8
16	+ 47	+ 72	36	+ 23	+ 44
17†	+109	+111			
18	− 15	+114			
19	−107	− 40			
20	− 28	+ 45			

* S.f. component of double star.
† N.f. component of double star.
‡ Very close double star.
§ S.f. component of double star.

to reach the cluster-type variables during their minimum phases. Mainly for this reason, the photometric investigation of the cluster has been carried out by means of material obtained at the 100-inch reflector. Plates distributed over three seasons led to the discovery of 36 variable stars (Table I, Plate XVII*a*). The list should be fairly complete for distances greater than 40″ from the center, but no attempt was made to discover variables in the central burned-out area. The present data indicate that the cluster is to be regarded as moderately rich in variable stars.

PHOTOGRAPHIC STANDARD MAGNITUDES FOR NGC 2419

Since provisional estimates showed that the cluster-type variables in NGC 2419 vary somewhere between magnitudes 18.5 and 20.0, the question of faint photometric standards became a matter of considerable importance. At present the Polar Sequence includes the only available standards of the requisite faintness. This sequence is not, however, accessible to the 100-inch reflector, owing to the peculiar mounting of the instrument. The other possibility—intercomparison of NGC 2419 and the polar standards with the 60-inch reflector—appeared unsatisfactory for two reasons: (1) Long exposures, of at least an hour's duration, would be necessary to reach the faintest stars needed in the investigation. Even if a rotating plateholder is used for such exposures, there is always some danger that the rotation of the field due to maladjustment of the polar axis is not compensated completely. Experience has shown that the peculiar structure of the images of the polar stars caused by a small residual rotation is likely to introduce marked scale deviations into intercomparisons with other fields. (2) On plates taken at the 60-inch reflector which extend to the lower limit of variation of the cluster-type variables, the stars in NGC 2419 are so densely crowded together that it would have been difficult to establish reliable sequences within the limits of the cluster itself.

To avoid these difficulties it was finally decided to extend the photographic scale in the nearby Selected Area 51 to magnitudes below 20. This phase of the work is a part of a larger program, now in progress at this Observatory, involving the extension of the photographic scale in a number of Selected Areas of the $+15°$ and $+30°$

PLATE XVII

a

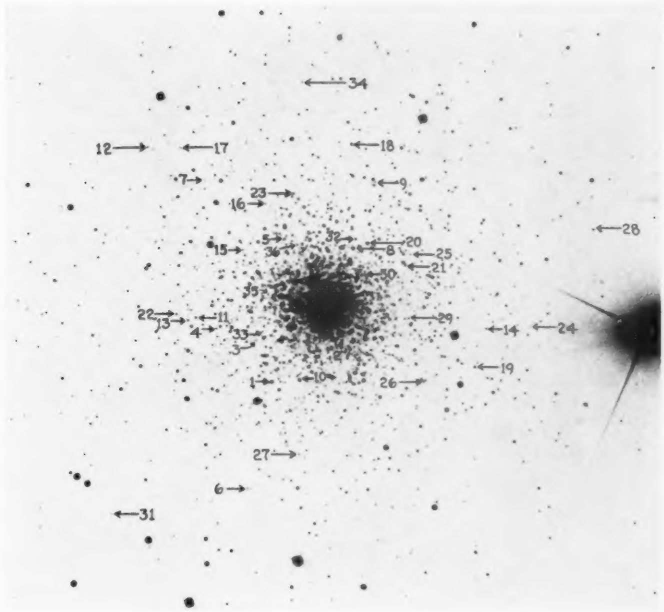

b

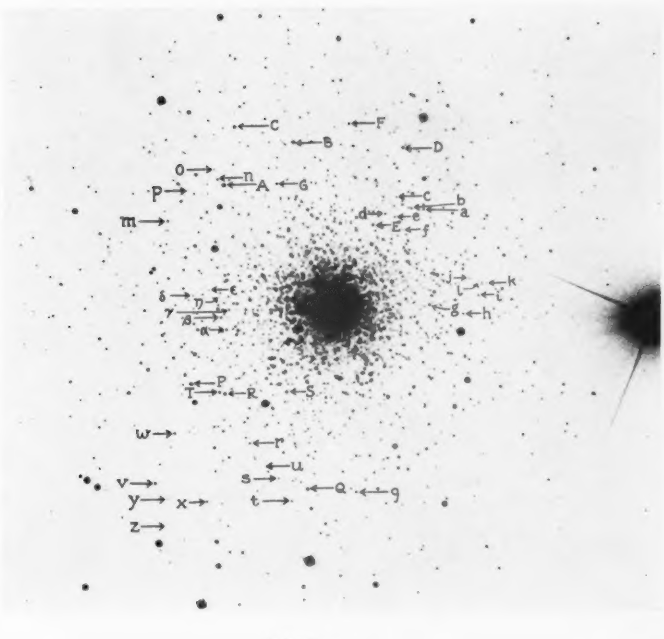

NGC 2419

(*a*) Variable stars; (*b*) comparison stars; scale, 1 mm = 5″.3

zones. Since the details of this investigation will be published later, a few general remarks may suffice at present. The observational method used in extending the scale is identical with that formerly employed by Seares in his photometric work, namely, the compari-

TABLE II

MAGNITUDES OF COMPARISON STARS IN NGC 2419

Star	Pg m	Residuals			Star	Pg m	Residuals		
		B 164	B 165	B 309			B 164	B 165	B 309
A	17.28	+8	−5	−3	m	18.51	−1	−4	+4
B	17.40	0	−3	+3	n	18.86	+1	−5	+5
C	17.69	+11	+1	−11	o	19.35	−3	......	+2
D	17.99	+11	−18	+6	p	20.07	......	......	
E	18.20	+6	−6	+1					
F	18.47	+2	0	−1	q	18.81	+1	−10	+9
G	18.68	0	−10	+10	r	18.94	−5	−11	+15
					s	19.19	−1	−1	+1
P	17.37	+9	−1	−8	t	19.42	−4	+4	+1
Q	17.73	+12	+5	−18	u	19.88	−2	......	+3
R	17.86	+9	−10	0					
S	18.31	−6	−4	+11	v	18.47	+6	+1	−8
T	18.49	−6	−3	+8	w	18.89	−1	+1	0
					x	19.26	+5	−4	−1
a	18.48	+4	+1	−4	y	19.63	−17	......	+17
b	18.59	−5	−11	+16	z	20.10	......	......	
c	18.89	+1	−8	+7					
d	19.07	+11	−9	−2	α	18.50	+3	−2	−1
e	19.28	−3	−6	+9	β	18.70	−7	−4	+12
f	20.07	......	......		γ	18.96	−3	+1	+2
					δ	19.25	+9	−6	−3
g	18.58	−4	−1	+6	ε	19.69	+3	+5	−9
h	18.76	0	−3	+4	η	20.21	......	......	
i	19.12	+6	−7	+2					
j	19.43	−3	−1	+4					
k	19.77	+7	......	−7					
l	20.20	......	......						

son of diaphragmed and undiaphragmed exposures with the Mount Wilson reflectors; so, also, is the method of reduction.

Since preliminary tests have shown that the photographic scale in the Selected Areas[3] is very well established to magnitudes 17.0–17.5, the extension is from 17.0 downward. One-hour exposures for each set of images at the 60-inch reflector allow an extension from magnitude 17.0 to about 19.4; at the 100-inch reflector, from 17.0 to about

[3] Seares and others, *Mt. W. Cat. of Sel. Areas, Carnegie Inst. Pub.*, No. 402, 1930.

20.4. Series with the two instruments therefore overlap nearly 2.5 mag. The complete material for each Selected Area consists of three such plates taken at each instrument. Although the material for S.A. 51 is not yet quite complete—three 60-inch and two 100-inch plates have been obtained—it is very improbable that the final values will differ sensibly from those adopted for the present investigation.

By means of three intercomparisons with S.A. 51 at the 100-inch reflector, a number of photometric sequences were established in NGC 2419. The resulting magnitudes are listed in Table II. For easy identification the comparison stars are marked on Plate XVII*b*. The considerable number of sequences is not only a convenience; comparison stars close to the variables are an essential if systematic errors due to differential coma are to be avoided. For the intercomparisons with S.A. 51 such errors were reduced to negligible amounts by using an 84-inch diaphragm, and the sequences should therefore be homogeneous in respect to zero point and scale value.

MEDIAN BRIGHTNESS OF THE CLUSTER-TYPE VARIABLES AND DISTANCE MODULUS OF NGC 2419

The observed magnitudes of the variables are collected in Table III. No attempt has been made to derive light-curves of the variables from the present material. For this purpose the distribution of the plates is rather unfavorable, owing to the fact that the cluster comes into opposition during the winter months, when inferior seeing conditions often make it impossible to obtain usable plates of such a difficult object. But for the present purpose of determining the distance of the cluster, light-curves of the variables are unnecessary, if we can make certain that the variables used are of the cluster type and if we can determine with sufficient accuracy their maximum and minimum magnitudes. Several consecutive plates during the same night are usually sufficient to reveal the characteristic behavior of the cluster-type variables with large amplitudes; and after the identification of a few typical cases, it is not difficult to segregate the whole group of variables of this type, since the dispersion in their median brightness is known to be remarkably small.[4] Thus the data

[4] E. Grosse, *A.N.*, **249**, 390, 1933.

in Table III are sufficient to show that all the variables listed belong to the cluster type, except Nos. 1, 8, 10, 18, and 20, which on the average are 1.3 mag. brighter than the others and will be discussed later.

To obtain the maximum and minimum brightness of the cluster-type variables the simplest procedure would be, of course, to read from Table III the extreme values for each variable. Precautions are necessary, however, to avoid two sources of error which tend to make the median brightness derived in this or in any similar way systematically too faint. One is incomplete observation of the maxima.

TABLE III

PHOTOGRAPHIC MAGNITUDES OF VARIABLES IN NGC 2419

Helioc. G.M.T.	Plate	1	3	4	5	6	7	8	9	10	11
2420000d+											
4172d752....	H 524	18.32	18.88	18.85	....	19.12	19.54	18.10	19.63	17.75	19.02
6688.795....	6	17.62	19.84	18.93	19.62	19.31	18.72	17.64	18.57	17.84	18.54
688.855....	7	17.55	<19.7	18.83	19.69	19.67	18.94	17.62	18.67	17.79	18.82
689.041....	9*	17.61	19.89	19.89	18.76	18.93	19.73	17.56	19.70	17.83	19.82
707.976....	15	18.33	18.83	......	<19.3	18.82	19.76	17.97	19.66	17.82	<19.2
708.028....	16	18.37	18.90	......	<19.3	18.90	<19.3	17.93	.....	17.92	<19.2
715.780....	17*	18.36	19.50	19.10	19.06	18.94	18.67	18.07	19.77	17.85	19.50
715.923....	18	18.37	19.55	19.02	18.85	19.18	19.31	18.13	18.80	18.02	18.90
715.980....	19	18.33	<19.7	19.17	18.71	19.39	19.46	18.16	.....	17.94	19.05
749.912....	23	17.60	18.80	19.20	19.41	19.36	19.86	17.65	19.70	17.36	19.68
749.961....	24	17.62	18.93	......	....	18.90	....	17.57	.....	17.46	<19.2
750.897....	30	17.59	<19.7	19.13	19.26:	19.53	18.66	17.54	.....	17.55	19.55
768.649....	32	17.66	18.60	19.57	19.20:	19.19	19.41	17.85	.....	17.77	19.52
768.766....	33	17.61	19.01	18.90	19.20:	19.41	19.62	17.89	.....	17.77	....
769.784....	39	17.66	19.55	......	18.75	19.28	19.01	17.62	.....	17.72	19.50
797.697....	42*	18.22	19.89	19.53	19.52	19.41	19.59	17.99	19.59	17.92	19.13
798.713....	52*	18.29	18.73	19.10	18.92	18.94	19.23	17.99	19.73	17.79	19.73
799.672....	58*	18.28	19.62	19.79	19.51	19.74	19.69	17.70	18.94	17.49	19.97
826.672....	62	17.54	19.73	19.70	19.29	19.17	19.38	17.84	.....	17.60	18.59
959.989....	143*	18.02	19.64	19.66	18.78	18.95	19.41	17.84	20.03	17.72	19.09
985.006....	148*	17.65	20.07	19.18	19.80†	19.36	18.98	18.09	19.59	17.64	19.66
985.988....	152*	17.62	19.57	19.07	19.65†	19.07	19.69	18.06	19.06	17.55	19.22
6986.976....	155*	17.61	19.91	19.53	19.22	19.42	19.29	17.97	19.48	17.61	18.63
7007.953....	159*	17.92	19.50	19.10	19.25	19.07	19.66	17.99	18.63	17.88	20.00
007.986....	160*	18.16	19.68	19.20	19.08	19.15	19.76	17.97	18.71	17.96	19.76
008.941....	164*	17.82	19.71	19.57	19.69†	19.57	19.31	18.12	19.73	17.82	19.33
008.973....	165*	18.04	19.94	19.64	19.38	19.28	19.48	18.06	19.55	17.86	19.62
033.853....	1439	17.68	19.97	19.03	19.22	19.55	18.69	17.63	18.92	17.64	19.84
035.025....	1445*	17.73	19.59	18.91	19.41	18.93	19.65	17.65	18.57	17.70	19.57
035.844....	1448	17.77	19.35	19.23	19.62	19.36	19.15	17.75	19.51	17.71	18.96
064.763....	179*	17.66	18.83	19.44	19.48	19.05	19.52	18.01	18.77	17.61	18.47
064.981....	182*	17.70	19.76	19.50	18.87	19.48	19.62	18.19	19.59	17.68	19.68
152.661....	183	17.80	....	19.02	19.25	19.59	19.62	17.67	19.33	17.60	18.93
370.011....	294*	17.84	19.97	19.21	19.10	19.32	19.83	18.07	19.59	17.85	19.10
391.879....	298*	17.81	19.97	19.00	19.76†	19.08	19.76	17.80	19.66	17.34	18.71
392.911....	303*	17.77	19.59:	19.57	18.76	19.11	19.55	17.80	18.80	17.28	19.59
393.883....	309*	17.83	20.02	19.10	19.69†	19.50	19.48	17.64	19.85	17.27	19.55
417.800....	313*	17.92	18.84	19.16	18.83	19.05	18.80	18.11	19.63	17.61	18.59
508.754....	343*	17.76	19.55	19.33	19.27	19.69	18.77	18.12	19.66	17.84	19.37
7721.965....	420*	17.81	19.79	19.52	19.25	19.69	19.83	17.38	19.63	17.44	18.97

* The limiting magnitude for the plate is below 20.0.

† Var. No. 5 has a faint companion, the light of which influences the estimates during the minimum phase. Only for those cases marked with a dagger was the variable well separated from its companion during this phase.

TABLE III—*Continued*

Helioc. G.M.T.	Plate	12	13	14	15	16	17	18	19	20	21	22
2420000ᵈ+												
4172ᵈ752...	H 524	19.69	19.50	19.06	19.50	20.04	19.58	18.37	19.43	18.08	18.86	19.81
6688.795...	6	18.59	18.77	19.25	19.15	20.01	18.85	18.30	19.58	17.96	19.51	19.97
688.855...	7	18.96	19.03	19.24	18.60	19.88	19.10	18.28	19.61	18.08	19.55	19.40
689.041...	9*	19.34	19.46	19.38	19.20	19.12	19.65	18.35	19.01	17.93	19.51	19.17
707.976...	15	18.78	18.74	.....	.....	19.83	19.78	18.33	19.40	18.06	19.51	18.83
708.028...	16	.....	18.65	.....	.....	.....	.....	18.37	....	18.05	.....	18.88
715.780...	17*	19.79	19.24	19.20	18.76	19.50	19.62	18.34	18.80	17.64	20.03	19.50
715.923...	18	18.80	19.64	19.54	19.17	19.93	19.03	18.35	19.36	17.65	20.03	19.84
715.980...	19	18.75	....	19.27	19.13	.....	18.72	18.39	<19.4	17.78	.....	....
749.912...	23	19.60	19.53	19.52	19.76	19.78	19.59	17.85	19.61	18.14	19.25	19.97
749.961...	24	.....	....	.....	.....	.....	19.60	17.83	....	17.99	.....	<19.7
750.897...	30	19.51	18.93	18.80	18.63	18.92	19.58	18.42	18.86	18.06	19.33	19.28
768.649...	32	19.59	<19.7	18.87	.....	19.62	19.01	18.37	19.29	17.93	.....	19.50
768.766...	33	19.62	18.45	18.94	19.19	20.04	19.12	18.12	<19.4	17.91:	.....	19.21
769.784...	39	.....	<19.7	.....	19.59	19.73	19.62	18.41	....	17.88	.....	....
797.697...	42*	19.62	19.17	18.98	19.16	19.55	19.25	18.28	19.73	18.03	18.74	18.83
798.713...	52*	18.74	19.73	19.58	19.76	19.87	19.34	18.18	18.88	17.99	19.55	19.59
799.672...	58*	19.62	19.12	19.61	19.04	19.38	18.75	18.40	19.41	17.90	19.63	19.82
826.672...	62	19.12	19.79	19.27	19.97	19.79	19.45	18.54	19.37	18.03	.....	19.97
959.989...	143*	19.66	19.48	18.83	19.84	18.82	18.73	17.99	19.86	17.84	19.65	18.78
985.006...	148*	19.76	19.35	19.67	19.81	19.93	19.73	18.07	19.27	18.03	18.84	19.62
985.988...	152*	18.82	19.19	18.96	19.24	18.81	18.82	18.50	19.34	18.12	19.73	19.05
6986.976...	155*	19.55	19.48	19.32	19.57	19.80	19.55	18.12	18.84	18.11	19.28	19.57
7007.953...	159*	19.23	19.84	19.40	19.46	19.03	19.69	18.48	19.88	17.69	19.28	19.24
007.986...	160*	19.41	19.73	19.61	19.84	18.74	19.20	18.46	19.40	17.78	19.40	19.45
008.941...	164*	19.69	19.00	18.99	19.05	19.51	19.69	17.97	19.24	17.88	19.55	18.88
008.973...	165*	19.62	19.18	19.00	19.12	19.76	19.69	18.10	19.39	17.79	18.97	18.51
033.853...	1439	19.58	18.73	19.69	18.74	19.76	19.55	18.36	<19.8	18.23	19.29	18.94
035.025...	1445*	19.08	19.52	19.27	19.28	19.83	19.69	18.47	19.80	18.18	19.25	19.46
035.844...	1448	19.83	19.08	19.39	19.05	19.83	19.80	18.08	19.88:	18.18	18.84	19.79
064.763...	179*	18.79	19.35	19.40	19.37	19.52	19.70	18.40	19.90	18.03	19.48	19.86
064.981...	182*	19.29	19.91	19.61	19.68	19.76	19.69	18.53	18.74	17.90	19.66	18.94
152.661...	183	19.40	19.57	19.03	19.50	19.29	19.80	18.15	20.00	17.97	19.26	19.26
370.011...	294*	19.29	18.90	19.03	19.50	19.79	19.83	18.56	18.98	17.60	19.27	19.13
391.879...	298*	19.41	19.20	19.61	19.55	19.38	19.69	18.52	19.39	18.15	18.82	18.68
392.911...	303*	19.66	19.59	18.90	18.74	19.72	18.49	18.33	19.43	17.93	19.70	19.66
393.883...	309*	19.38	19.52	19.27	19.81	19.76	19.65	17.99	19.00	18.07	18.72	19.91
417.800...	313*	19.69	19.84	19.56	18.63	19.59	19.62	18.09	19.31	17.87	19.77	18.69
508.754...	343*	19.01	19.61	19.32	19.15	19.80	19.83	18.55	19.39	18.17	19.48	19.89
7721.965...	420*	19.06	19.66	19.40	19.16	19.83	18.96	18.54	18.98	17.60	18.89	19.66

The only remedy for this is to omit all variables for which any doubt exists as to whether the maximum has been properly covered by observations. Minimum phases are usually well represented even with limited material, but the dispersion of the observational errors is a second source of systematic error. Especially in the present case, where the minimum magnitudes are close to the plate limit, the dispersion to be expected in the observational errors is considerable and influences appreciably the minimum brightness, even when derived from the 6 to 10 faintest magnitudes of any variable in Table III. To minimize, as far as possible, the effects of this systematic error, two ways are open: either derive the value of minimum brightness from observations distributed over a range so large that the observational errors cancel out, or else use only plates of high quality for

TABLE III—*Continued*

Helioc. G.M.T.	Plate	24	25	27	28	29	31	32	33	34	35	36
$2420000^{\rm d}+$												
$4172^{\rm d}752$...	H 524	19.18	18.94	19.10	19.61	....	19.16	19.27	19.52	19.34	......	.....
6688.795...	6	19.20	19.01	19.27	19.40	....	19.19	19.11	20.13	19.90	20.00	19.83
688.855...	7	.....	19.22	19.17	19.65	....	19.17	19.24	19.22	19.62	20.02	19.83
689.041...	9*	19.52	19.77	19.29	19.82	19.92	19.36	19.48	19.57	19.22	20.00	19.12
707.976...	15	.....	.....	19.57	18.88	<19.4	19.00:	18.84	19.14	19.55:	......	.....
708.028...	16	.....	.....	19.40	.....	....	19.66:	.....	.....	.....	......	.....
715.780...	17*	19.16	19.44	19.33	18.98	19.37	19.50	19.21	19.20	19.69	19.67	19.62
715.923...	18	19.38	19.63	19.11	19.50	19.63	19.49	19.70	19.89	19.45	19.97	19.77
715.980...	19	19.63	.....	19.11	19.65	....	19.27	.....	......	19.10	......	.....
749.912...	23	19.53	19.21	19.39	18.98	19.65	19.52	19.36	19.76	19.03	19.92	19.41
749.961...	24	.....	.....	19.19	19.10	....	.....	.....	.....	.....	......	.....
750.897...	30	19.20	19.51	19.50	19.38	19.22	19.04	18.86	19.18	19.62	19.20	19.55
768.649...	32	.....	.....	19.09	18.99	19.29	19.49	.....	19.24	19.79	......	.....
768.766...	33	19.36	19.48	19.36	18.96	....	19.08	.....	19.17	19.55	......	.....
769.784...	39	.....	.....	19.11	.....	....	.....	.....	.....	.....	......	.....
797.697...	42*	19.00	19.22	19.66	19.67	19.43	19.55	19.70	19.58	19.45	19.40	19.76
798.713...	52*	19.43	19.28	19.41	19.47	19.34	19.27	19.48	19.17	19.25	19.91	19.72
799.672...	58*	18.93	19.55	19.16	19.43	19.01	19.43	19.49	19.66	19.58	19.48	19.65
826.672...	62	19.31	19.40	19.61	19.31	19.17:	19.59	.....	19.22	19.17	18.88	19.72
959.989...	143*	19.54	19.57	19.28	19.84	19.06	19.44	19.85	19.48	19.45	18.93	19.10
985.006...	148*	19.02	19.81	19.16	19.86	19.37	19.20	19.40	19.28	19.69	19.79	19.97
985.988...	152*	19.47	19.03	19.28	19.03	19.23	19.29	18.72	19.66	18.98	19.59	19.48
6986.976...	155*	19.03	19.81	19.71	19.84	19.26	19.16	19.51	19.19	19.65	19.97	19.90
7007.953...	159*	19.15	19.44	19.13	18.90	19.35	19.23	19.03	19.11	19.77	20.00	19.29
007.986...	160*	19.35	19.33	19.15	18.90	19.37	19.29	19.02	19.21	19.58	19.94	19.25
008.941...	164*	19.40	19.12	19.26	19.36	19.45	19.41	19.66	19.44	19.01	19.61	19.69
008.973...	165*	19.52	19.44	19.42	19.54	19.47	19.11	19.63	19.66	19.10	19.58	19.69
033.853...	1439	19.62	19.66	19.50	19.03:	19.36	19.17	19.70	19.21	19.41	18.87	19.06
035.025...	1445*	19.41	19.06	19.15	19.08	19.61	19.23	19.25	19.50	19.69	19.68:	19.79
035.844...	1448	.....	.....	19.22	19.28	19.84	19.21	19.59	......	19.68	......	19.41
064.763...	179*	19.26	18.74	19.15	19.00	19.73	19.41	19.48	19.37:	19.45	19.97	19.83
064.981...	182*	19.63	19.44	19.37	19.10	19.61	19.47	18.58	19.55	19.10	18.88	19.10
152.661...	183	19.40	19.01	19.37	19.56	19.56	19.63	19.24	19.40	19.17	19.94	19.66
370.011...	294*	19.67	19.63	19.27	18.71	19.33	19.34	18.80	19.55	19.42	19.59	19.72
391.879...	298*	19.37	19.01	19.17	19.34	19.36	19.18	18.74	19.66	19.25	19.62	19.54
392.911...	303*	19.34	19.59	19.37	19.67	19.90:	19.61	19.24	......	19.38	19.64	19.69
393.883...	309*	19.61	19.36	19.26	18.73	19.08	19.10	18.99	19.57	19.44	19.86	19.69
417.800...	313*	18.90	19.51	19.21	18.82	19.05	19.27	19.20	19.76	19.20	19.08	19.76
508.754...	343*	19.37	19.66	19.55	19.76	19.88	19.47	18.49	19.52	19.31	19.89	19.83
7721.965...	420*	18.98	19.66	.....	19.37	19.34	19.47	18.84	19.68	19.65	19.09	19.69

which the dispersion due to observational errors is small. In the present case the latter procedure has been adopted, and only those plates have been used for deriving minimum magnitudes on which the faintest comparison stars of Table III appear as well-exposed images. These plates are marked in Table III by asterisks.

The values derived for the maxima and minima of the cluster-type variables in NGC 2419 are given in Table IV, together with the amplitudes and the values for the median brightness. On the average, each maximum brightness is based on three individual values (two to four for different stars), each minimum brightness on seven values (five to eight). Components of close doubles and variables with insufficiently observed maxima have been omitted. As far as can be judged from Table IV, the procedure here adopted has worked well.

The amplitudes of the cluster-type variables show the normal range of from 0.45 to 1.30 mag., and the small dispersion in the absolute magnitudes is represented by the correspondingly small scatter of the values of the median brightness. With the customary value, $M = 0.0$,

TABLE IV

PHOTOMETRIC DATA FOR CLUSTER-TYPE VARIABLES IN NGC 2419

Var. No.	Max.	Min.	Ampl.	Med. m
3	18.66	19.96	1.30	19.31
4	18.84	19.65	0.81	19.24
5	18.75	19.72	0.97	19.23
6	18.86	19.64	0.78	19.25
7	18.69	19.77	1.08	19.23
9	18.59	19.76	1.17	19.18
11	18.55	19.81	1.26	19.18
12	18.69	19.71	1.02	19.20
13	18.55	19.75	1.20	19.15
14	18.81	19.62	0.81	19.22
15	18.62	19.76	1.14	19.19
16	18.77	19.85	1.08	19.31
17	18.65	19.75	1.10	19.20
19	18.77	19.86	1.09	19.32
21	18.76	19.74	0.98	19.25
22	18.60	19.84	1.24	19.22
24	18.94	19.58	0.64	19.26
27	19.10	19.55	0.45	19.33
28	18.72	19.78	1.06	19.25
31	19.08	19.53	0.45	19.31
32	18.60	19.71	1.11	19.16
34	19.00	19.66	0.66	19.33
37	18.78	19.70	0.92	19.24

for the median absolute magnitude of the cluster-type variables, the distance modulus of NGC 2419 as derived from the data in Table IV is

$$m - M = 19.24 \pm 0.01 \text{ (M.E.)} .$$

BRIGHT IRREGULAR VARIABLES IN NGC 2419

The data for the five bright variables found in NGC 2419 are collected in Table V. The amplitudes are of small or intermediate range. All attempts to derive light-elements for these variables from the present material have been unsuccessful, and the indications are

that their light fluctuates irregularly. Judged by a qualitative comparison of their magnitudes on photographic and photovisual plates, the variables probably belong to spectral types G to K. Since irregular variables are seldom found in globular clusters, this group of bright variables in NGC 2419 deserves further attention.

TABLE V

PHOTOMETRIC DATA FOR BRIGHT VARIABLES IN NGC 2419

Var. No.	Max.	Min.	Ampl.	Med. m	Pg M
1	17.59	18.32	0.73	17.95	−1.29
8	17.50	18.10	.60	17.80	1.44
10	17.31	17.93	.62	17.62	1.62
18	17.84	18.53	.69	18.19	1.05
20	17.65	18.16	0.51	17.90	−1.34

DISTANCE MODULUS DERIVED FROM THE 25 BRIGHTEST STARS

Although the distance modulus of NGC 2419 derived from the cluster-type variables should meet all requirements, it appeared desirable, nevertheless, to obtain some check by another method. For this purpose the method of the 25 brightest stars is well adapted, since it affords at least a rough test of the essential correctness of the faint photographic standards used for the cluster-type variables. About 50 of the brightest stars, well distributed over the whole cluster area, were therefore measured on plates of short exposure. The results were first used to fix the upper limit of luminosity for the cluster stars. By plotting the numbers of stars for successive intervals of brightness, it was found that the upper limit in apparent magnitude for cluster stars is 17.2, with an uncertainty of the order of 0.1 mag. The corresponding upper limit in absolute photographic magnitude is $M=-2.0$, in complete agreement with results obtained from other globular clusters. After excluding all stars brighter than magnitude 17.2 as field stars, the 25 brightest stars in NGC 2419 are those listed in Table VI. Their mean brightness is $\bar{m}_{25}=17.84$.

To reduce this value to the distance modulus, the cluster must be assigned to one of Shapley's classes. The available plates indicate a rich, condensed cluster of the very early classes for which Mod$-\bar{m}_{25}=+1.32$. Practically the same value results when NGC 2419 is

intercompared with a number of brighter globular clusters for which the reduction constant in question is well determined. It was thus

TABLE VI

MAGNITUDES OF THE 25 BRIGHTEST STARS

No.	Pg m	No.	Pg m
1	17.30	14	17.85
2	17.54	15	17.87
3	17.61	16	17.88
4	17.63	17	17.91
5	17.68	18	17.96
6	17.74	19	17.99
7	17.77	20	18.03
8	17.78	21	18.03
9	17.78	22	18.04
10	17.79	23	18.07
11	17.83	24	18.08
12	17.83	25	18.10
13	17.85		

found that in stellar content and structure NGC 2419 is very similar indeed to the following clusters:

	Mod $-\overline{m}_{25}$
M 3	+1.27
M 5	1.29
M 15	1.32
M 53	+1.46
Mean	+1.33

Moreover, it can be proved directly that NGC 2419 belongs among the richest globular clusters known in our galaxy. The integrated apparent brightness of NGC 2419 has recently been determined at this Observatory by Stebbins with a photoelectric cell, and by Christie with a schraffierkassette. Their unpublished values,[5] both on the photographic scale, are in close agreement:

$$m_t = 11.1 \text{ (Stebbins)} ,$$

$$m_t = 10.9 \text{ (Christie)} .$$

[5] I am much indebted to Dr. Stebbins and Mr. Christie for their kind permission to use their data.

With the modulus derived from the cluster-type variables the total absolute brightness of NGC 2419 becomes

$$M_t = -8.3 ,$$

a value which is independent of any obscuration affecting the measured values of the modulus and m_t. Although still to be considered provisional, Hubble's[6] frequency-curve of the absolute magnitudes for the globular clusters of our galactic system shows that their upper limit of luminosity is close to $M = -8$. NGC 2419 is therefore a cluster of high luminosity and consequently of rich stellar content, since, according to all indications, the luminosity function of the cluster stars is closely the same for all globular clusters.[7] Since both the general appearance of NGC 2419 and its absolute magnitude indicate a rich cluster of high luminosity, the reduction constant $+1.33$, corresponding to Shapley's classes I–III, has been adopted. We therefore obtain as modulus of the cluster from the 25 brightest stars 19.17, in close agreement with the value derived from the cluster-type variables. Assigning weights 3 and 1 to the two determinations, we obtain as the final distance modulus of NGC 2419

$$m - M = 19.22 ,$$

corresponding to a distance of 69,800 parsecs.

TESTS FOR LOCAL OBSCURATION IN THE FIELD OF NGC 2419

The foregoing result is by far the largest distance obtained for any globular cluster in our galactic system. In view of its implications, which would place NGC 2419, detached from the rest of the globular clusters, far out in intergalactic space, it is necessary to determine whether our photometric results have been influenced by local absorption in the neighborhood of the cluster, whose galactic coordinates are $l = 148°$, $b = +27°$. Hubble's investigations[8] show that in this anticenter region of our system the zone of obscuration nar-

[6] *Mt. W. Contr.*, No. 452; *Ap. J.*, **76**, 97, 1932.

[7] The total luminosity would seem to be the logical characteristic for a classification of the globular clusters. Shapley's characteristic—the apparent central concentration of a cluster—is impractical and often misleading, since it depends on the distances of the clusters.

[8] *Mt. W. Contr.*, No. 485; *Ap. J.*, **79**, 8, 1934.

rows down to its smallest extent, especially for northern galactic latitudes. A closer inspection of Hubble's maps shows indeed that between longitudes 130° and 180° the distribution of nebulae is normal and unaffected by local obscuration for all latitudes higher than +20°. The surrounding field of NGC 2419 was specially examined by counting the nebulae on two Eastman 40 plates of 1-hour exposure taken at the 100-inch reflector. The number of nebulae found ($N=54$) is practically identical with the average number for high galactic latitudes. That the area of the cluster itself forms no exception is shown by the fact that eight of these nebulae are situated within its boundaries, at distances $<3\rlap{.}'6$ from the center of the cluster.

Moreover, there are no indications of any selective absorption in the integrated light of NGC 2419. The color index of the cluster, measured photoelectrically by J. Stebbins,[9] indicates that it belongs to color class $f2\pm3$ (P.E.). A very good spectrogram of the right density, obtained by the writer with 16 hours' exposure on January 14–15, 1934, with the 60-inch telescope and the two-prism Rayton-lens spectrograph, was classified by Mr. Humason as F5. Color class and spectral type therefore agree as closely as one can expect. Altogether, the foregoing results leave no doubt that NGC 2419 is situated in a normal field outside the zone of local obscuration.

INFLUENCE OF THE GENERAL GALACTIC ABSORPTION (LATITUDE EFFECT)

How far the photometric distance is influenced by the general latitude effect can be answered only approximately at present. According to Hubble's cosecant law,[8] all photometric distances must be multiplied by the factor f, given by the relation

$$\log f = -0.05\ |\operatorname{cosec} b|\ ,$$

to free them from the influence of absorption. For NGC 2419, $f=0.77$, giving a reduction of 23 per cent in the photometric distance. This value of f is, however, probably a lower limit, because the absorption in the anticenter zone between $b=+20°$ to $+30°$ is less than that indicated by the simple cosecant law in which the dependence

[9] *Mt. W. Comm.*, No. 111; *Proc. Nat. Acad.*, **19**, 222, 1933.

upon longitude has been neglected. As far as can be inferred from the available data, the true value probably lies between 0.77 and 0.85. In the following, $f=0.80$ has been adopted, which corresponds closely to the mean of the determinations of the absorption constant by Hubble ($\Delta m_{\mathrm{Pole}}=0.25$) and by Stebbins ($\Delta m_{\mathrm{Pole}}=0.21$).

A distance factor of this order also brings the somewhat excessive value for the linear diameter of the cluster within the normal range. By tracing the cluster stars on long exposures out to where they merge into the field density of the foreground stars, an angular diameter of 7.′2 was found as the mean of several determinations. The resulting linear diameter is 147 parsecs, if the latitude correction be omitted, whereas, with the factor suggested, it would be reduced to 117 parsecs. For comparison, the linear diameters of the four clusters already mentioned have been derived in the same way with the following results:[10]

	Corrected for Latitude Effect
M 3	124 parsecs
5	95
15	86
53	109

The corrected linear dimensions of NGC 2419 are therefore comparable with those of similar clusters.

THE RESULTS

The results derived so far are summarized in Table VII. In computing the distance of NGC 2419 from the center of the galactic system, 10,000 parsecs has been adopted as the distance of the sun from the center of the system. The radial velocity was derived from the spectrogram already mentioned.

The detached position of NGC 2419 relative to the rest of the globular clusters is well illustrated in Figure 1, which represents the projection of the system of clusters on the X,Z plane, in which NGC 2419 is situated. All distances have been corrected for the latitude effect. A solution of this kind probably represents only a very rough approximation for the complicated cases of clusters in

[10] Diameters of the same order are obtained if the outlying cluster-type variables are used to define the dimensions of the clusters.

low latitudes (small values of $|Z|$); but it should nevertheless lead to pretty definite information regarding the dimensions of the system

TABLE VII

SUMMARY OF RESULTS

	Measured	Corrected for Lat. Effect
Modulus, $m-M$	19.22 mag.	18.75 mag.
Distance from sun	69,800 parsecs	55,800 parsecs
Distance from center of galaxy	78,900 parsecs	64,300 parsecs
Apparent diameter	7!2	
Linear diameter	147 parsecs	117 parsecs
Apparent total brightness:		
a) Photoelectric (Stebbins)	11.1 mag.	
b) Photographic (Christie)	10.9 mag.	
Absolute total brightness	− 8.2 pg M	
Upper limit of luminosity for stars	− 2.0 pg M	
Color class (Stebbins)	f 2	
Spectral type (integrated spectrum)	F5	
Radial velocity	+20 km/sec	

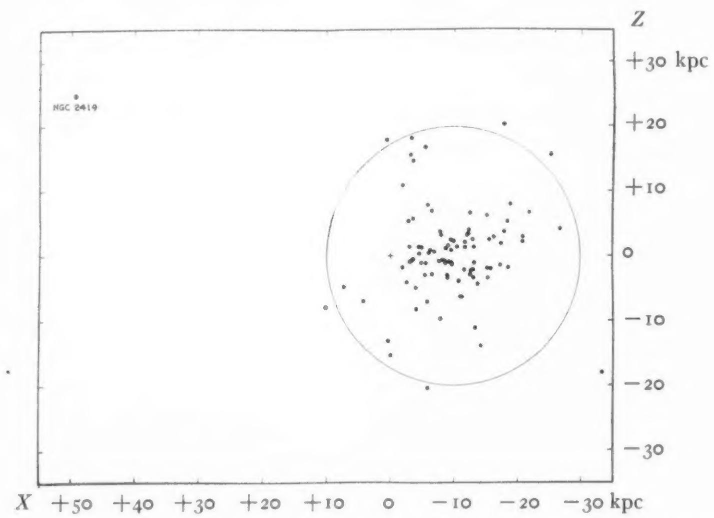

FIG. 1.—The system of globular clusters projected on the X, Z plane. The distances have been corrected for the latitude effect ($\Delta m_{\mathrm{Pole}} = 0.23$).

of globular clusters. Figure 1 shows that practically all globular clusters are contained within a sphere of 20,000 parsecs radius

around the center of the Milky Way system. The only important exceptions are NGC 7006[11] and NGC 2419, with distances of 37.9 and 64.3 kpc, respectively. That the distance of NGC 2419 from the center of our system is a considerable fraction of the corresponding distances of the nearest extra-galactic systems is finally shown by the figures in Table VIII.

In view of the large distance, it has been suggested that NGC 2419 might be an independent intergalactic object. For dynamical reasons we should then expect that the space velocity of NGC 2419 would be larger than the velocity of escape. Unfortunately, we know

TABLE VIII

Object	Distance from Center of Galaxy (Corrected for Latitude Effect)
NGC 2419	64.3 kpc
S.M.C.	23.3
L.M.C.	22.5
NGC 6822	153
M 31	216
M 33	224

only one of the three velocity components, the radial velocity. Even so, we should be certain that the cluster cannot be a member of our galaxy if

$$|v_{\mathrm{red}}| > V_e \, , \qquad (1)$$

where v_{red} is the radial velocity of the cluster reduced to the center of the galaxy and V_e the parabolic velocity at the distance of NGC 2419. Adopting as the orbital velocity of the sun $v = 280$ km/sec in the direction $l = 55°$, $b = 0°$, and as radius vector $r = 10$ kpc, we obtain $v_{\mathrm{red}} = +9$ km/sec and $V_e = 156$ km/sec. The inequality (1) is therefore certainly not fulfilled. Since (1) is a sufficient but not a necessary condition, the matter is left indeterminate as far as our present argument is concerned. On the other hand, the argument that the distance of NGC 2419 is comparable with those of the nearest extra-

[11] The distance of NGC 7006 is somewhat uncertain. Dr. Hubble informs me that, according to his measures, Shapley's magnitudes in this cluster need a systematic correction of the order of -0.3 to -0.5. I have adopted $m - M = 18.6$ for the measured modulus.

galactic systems carries no great weight, since this special feature is largely due to the fact that our galaxy and the nearest extra-galactic systems form what may be termed a local group of nebulae. Within a sphere of 250 kpc radius around our galaxy we know at present nine extra-galactic systems: our galaxy, the two Magellanic Clouds, M 31 and its two companions, M 33, NGC 6822, and NGC I 1613.[12] The corresponding density is 2×10^{-16} nebulae per cubic parsec, or even twice this value, since the group occupies only the half-sphere south of the galactic plane. Since the nebular density for intergalactic space at large is of the order of 10^{-17} nebulae per cubic parsec, the density in our local group is twenty to forty times larger than normal; consequently, the average distance between neighboring systems is only one-third the normal value (normal, 580 kpc; group value, 190 kpc). Actually, some of the members are in rather close contact, e.g., our galaxy and the Magellanic Clouds for which $D < 25$ kpc; to a lesser degree, M 31 and M 33, for which $D = 56$ kpc. Under these circumstances neighboring systems with far-outlying members such as globular clusters and cluster-type variables will almost certainly overlap.

It therefore seems that the question whether globular clusters occur in intergalactic space as independent systems can be answered only by future discoveries. According to all indications, however, such cases must be rare indeed, if they occur at all.

Carnegie Institution of Washington
Mount Wilson Observatory
August 1935

[12] The modulus for this irregular system, which is under investigation at the Mount Wilson Observatory, is $m - M = 22.2$.

THE SPECTRUM OF NOVA HERCULIS λλ 5150–6550 A*

By PAUL W. MERRILL

ABSTRACT

Absorption lines.—Special attention was paid to the D lines of sodium, which were accurately measurable throughout a long interval. Other elements observed include *Ba* II, *O* I, *Si* II, *Fe* II, *Ti* II, *Sc* II, *Cr* II, *Y* II, and *He* I. Weak *Na* lines, probably interstellar, with displacements of −18 km/sec, were measured on a few of the early plates. The first group of displaced lines, called component I, with a displacement of about −180 km/sec, was observed until December 26, 1934 (Table I, Fig. 1). Component II persisted from December 23, 1934, to March 25, 1935, the displacement increasing from −280 to −395 km/sec (Table II, Fig. 2). Components I and II both were present from December 23.5 to December 26.1 G.M.T. Their relative behavior is described in detail. Lines of *Ba* II, although weak, behaved much like components I and II of *Na* I. Lines of *O* I were very intense at first in component I but were never conspicuous in component II. Numerous measurements were made of component II for *Na* I, *Ba* II, *Sc* II, *Ti* II, and *Fe* II. In addition to I and II, other components with much greater displacements were observed.

Emission lines.—The bright lines in the visual region are in general more outstanding and better suited to accurate measurement than those of shorter wave-lengths. Lines of *Fe* II, *O* I, *Si* II, *Na* I, and *H* associated with component I were of the P Cygni type. With the exception of *Hα* they were not of high intensity. Lines associated with component II became much more intense. At first flat-topped, with widths corresponding to about 540 km/sec, they next became saddle-shaped, and, finally, very unsymmetrical with the violet maxima the stronger. The widths increased to 700 or 800 km/sec. Numerous measurements made on the edges, maxima, and centers of several lines of *Fe* II, as well as of the auroral line, λ 5577, and the two red lines, λ 6300 and λ 6363, of [*O* I], are summarized in Tables IV, V, and VI. λ 5755 [*N* II], measured on a few spectrograms, was wider and less well defined than other emission lines.

Discussion.—Halm's hypothesis of an expanding atmosphere may take one of two forms, depending on whether the emission of atoms is assumed to be instantaneous or continuous. The chief facts concerning the widths and displacements of both bright and dark lines appear favorable to this hypothesis, although many details are puzzling. The comparative behavior of lines of *Fe* II and [*O* I] may largely be explained by the inability of the atoms in front of the star to produce forbidden lines in absorption. On this interpretation the radial velocity of the star as a whole was −4 km/sec, and the emitting and absorbing gaseous shell had a radius about twice that of the photosphere. The expanding atmosphere may arise from an explosive pulse which drives off matter in a condensed or quasi-liquid state from which gaseous atoms later evaporate.

In spectra having both emission and absorption lines the absorption lines are often relatively more conspicuous in the violet and ultra-violet regions, while the emission lines stand out more clearly toward the longer wave-lengths. This tendency, for which the quantum theory provides a general explanation, was well marked in the spectrum of Nova Herculis 1934, especially in the early history, and, combined with the presence of both permitted and forbidden lines,

* *Contributions from the Mount Wilson Observatory, Carnegie Institution of Washington*, No. 530.

gives special point to a study of the bright lines in the visual region. The Mount Wilson observations will therefore be reported in some detail. Among the absorption lines, those of sodium are of special interest, while those of *O* I, *Si* II, *Sc* II, *Ti* II, *Fe* II, and *Ba* II also were systematically measured.

Nearly all the Mount Wilson spectrograms of the visual region were made at the 100-inch telescope with the Cassegrain grating spectrograph[1] and 18-inch camera yielding a dispersion of 33.6 A/mm. The special panchromatic emulsions III C or III F made by the Eastman Kodak Company were employed.

It will be convenient to deal with the dark lines first.

ABSORPTION LINES

The dark lines may be divided into several distinct groups according to the displacements from their normal position. The first group, called "component I," having a displacement of about −180 km/sec, was present from December 18.6 (or earlier) to December 26.1 G.M.T. Component II, the most persistent of all, was measured on all suitable plates from December 23.6 to March 25.0, its displacement increasing meanwhile from −280 km/sec to −395 km/sec. Other components with much greater displacements and an apparently erratic behavior were observed on numerous plates. The general appearance of the spectrum on various dates is illustrated in Plates XVIII and XIX.

On the early plates, December 15.5 to December 22.5, the absorption lines correspond to those of α Cygni, but are wider and the edges are not quite so sharp. They present, nevertheless, excellent marks for measurement and yield accurate displacements. Their intensities, compared to those in α Cygni, were as follows:

Element	Intensities of Dark Lines Compared with α Cygni	Bright Components
Na	Same or weaker	Trace
Fe II, *Si* II	Somewhat stronger	Weak
O I	Much stronger	Weak

[1] *Mt. Wilson Contr.*, No. 432; *Ap. J.*, **74**, 188, 1931.

PLATE XVIII

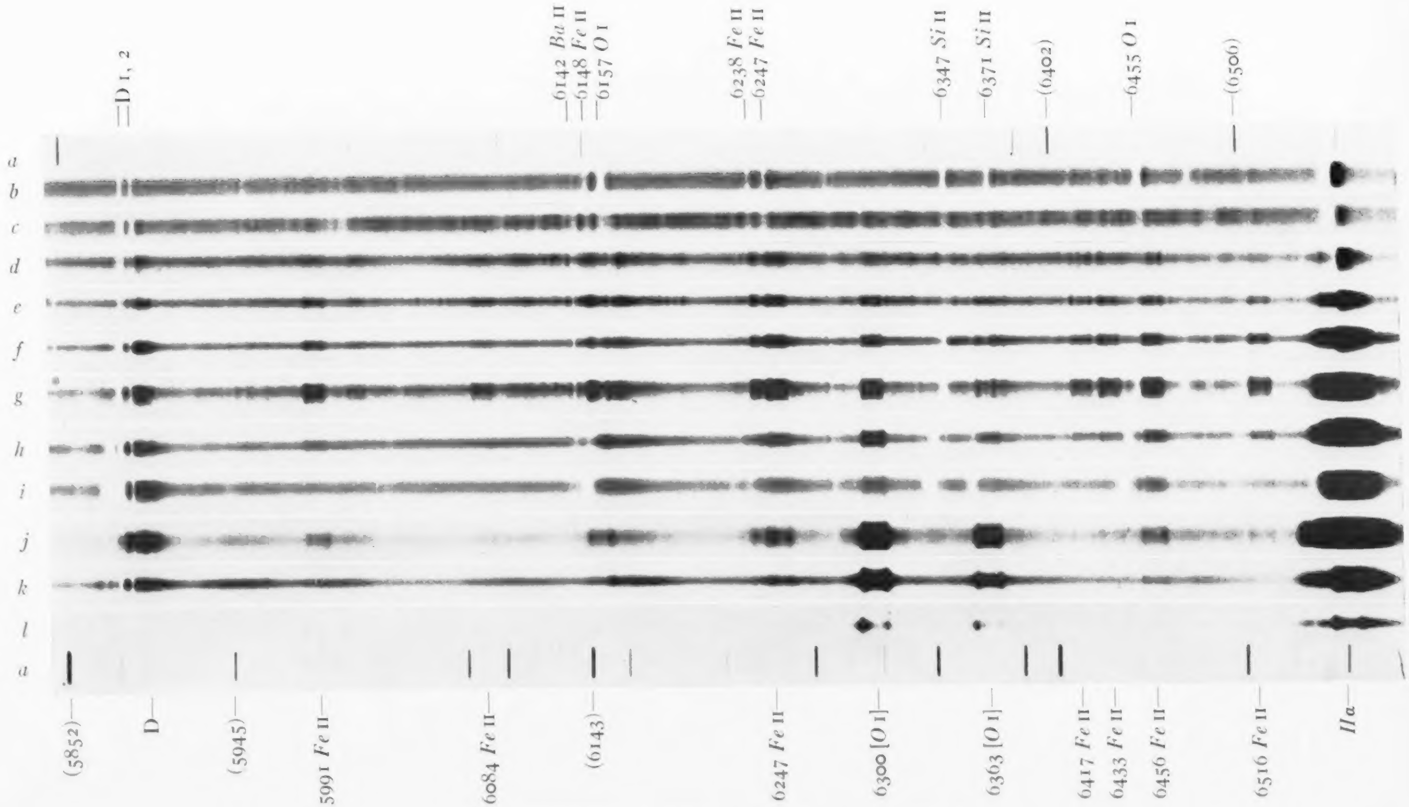

SPECTROGRAMS OF NOVA HERCULIS, REGION D–*Hα*

Absorption lines are marked above, emission lines below. (*a*) *Ne* comparison (wave-lengths in parentheses); (*b*) 1934, Dec. 21.6, G.M.T.; (*c*) Dec. 24.1; (*d*) Dec. 25.1; (*e*) Dec. 26.1; (*f*) Dec. 29.1; (*g*) Dec. 30.1; (*h*) 1935, Jan. 17.0; (*i*) Jan. 20.0 (*j*) Jan. 31.0; (*k*) Mar. 5.1; (*l*) Apr. 2.0.

PLATE XIX

PLATE XIX

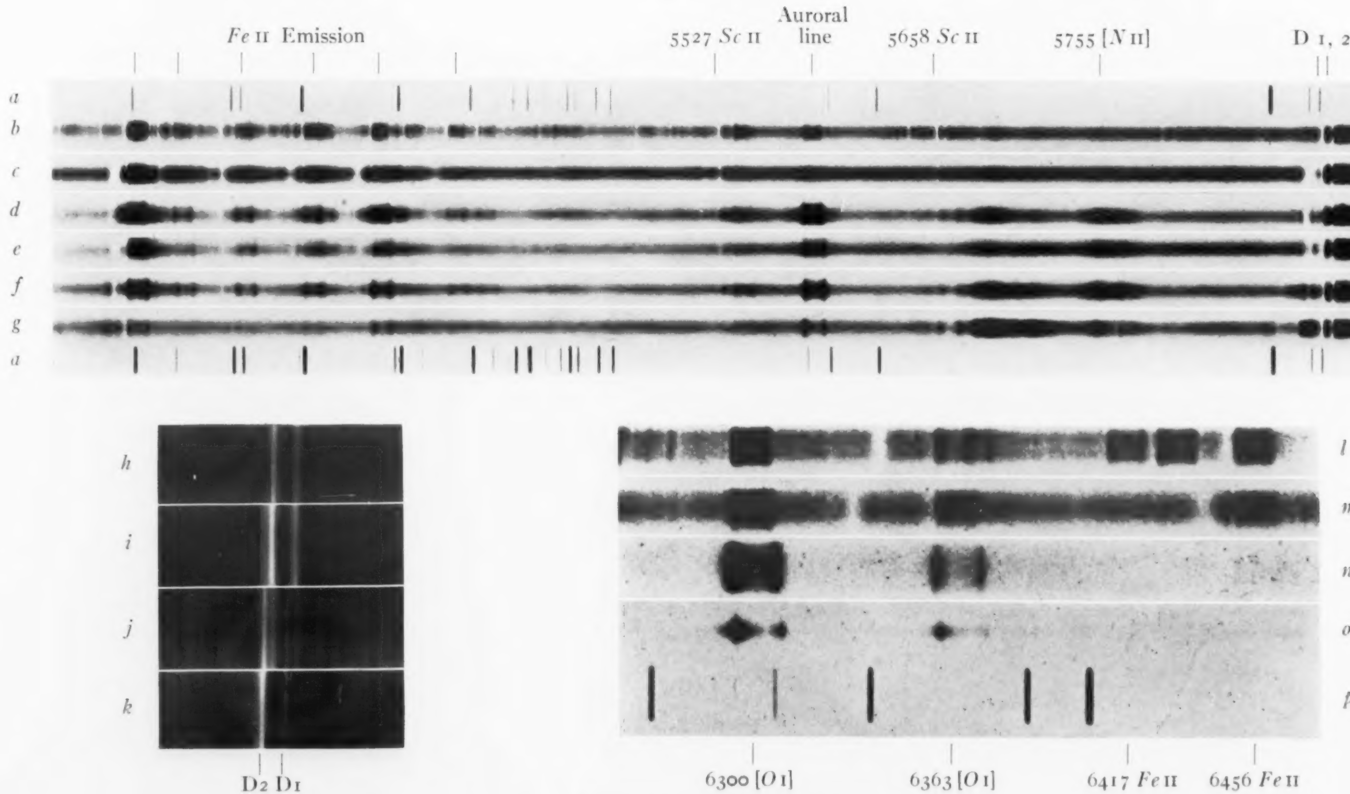

SPECTROGRAMS OF NOVA HERCULIS

Upper: Green and yellow region. (*a*) Comparison spectrum; first line, λ 5167; all lines from *Fe* arc except three at the extreme right, 5852 *Ne*, 5876 *He*, and 5882 *Ne*, respectively. (*b*) 1934, Dec. 31.1, G.M.T.; (*c*) 1935, Jan. 20.1; (*d*) Feb. 2.0; (*e*) Feb. 18.0; (*f*) Mar. 5.0; (*g*) Mar. 25.0. Lower left: artificially widened D lines; (*h*) component I, 1934, Dec. 22.6; (*i*) Dec. 24.1; (*j*) Dec. 25.6; (*k*) component II, Dec. 29.1. Lower right: [*O* I] and *Fe* II emission lines in the red; (*l*) Dec. 30.1; (*m*) 1935, Jan. 21.1; (*n*) Mar. 17.0; (*o*) Apr. 2.0; (*p*) *Ne* comparison, λλ 6266, 6305, 6334, 6383, 6402.

Component I was seen on December 26.1, but could not be detected on the next plate, taken on December 29.1. Component II first showed on December 23.5 and then rapidly increased in intensity; it was not seen on December 22.5. The observed period of simultaneous visibility of both components was therefore December 23.5 to December 26.1. The rapid changes of relative intensity of components I and II are best shown by the lines of sodium (Plate XIX) and of ionized barium. Lines of *O* I, *Si* II, and *Fe* II probably behaved in about the same way, but during the period of transition

TABLE I

DISPLACEMENTS OF ABSORPTION LINES IN KM/SEC
(Early Period; Component I Complete)

G.M.T.	D1, 2		*Ba* II		*O* I		*Si* II		*Fe* II
	Comp. I	Comp. II	Comp. I	Comp. II	Comp. I	Comp. II	Comp. I	Comp. II	Comp. I
1934 Dec. 18.55..	179* 2†	... ..	... ..	... ..	171 3	... ..	166 2	... ..	180 2
19.55..	175 4	... ..	... ..	... ..	166 4	... ..	161 4	... ..	176 5
21.09..	173 6	... ..	... ..	... ..	168 5	... ..	165 7	... ..	169 11
21.55..	172 12	... ..	... ..	... ..	166 11	... ..	161 13	... ..	170 20
22.56..	176 10	... ..	... ..	... ..	179 3	... ..	176 10	... ..	179 17
23.55..	182 10	276: 5	182 8	282 6	... ..	(203) 3	182 5	265 4	184 8
24.10..	191 10	289 8	195 7	281 9	... ..	(249) 1	... ..	(239) 1	... ..
24.56..	182 12	299 12	200 9	292 12	... ..	... ..	... ..	... ..	... ..
25.09..	184 10	312 10	189 6	314 9	... ..	... ..	... ..	... ..	... ..
25.56..	182 6	313 6	186 5	316 10	... ..	.. ..	... ..	... ..	... ..
26.09..	176 8	320 8	164: 1	319 8	... ..	... ..	... ..	... ..	... ..

* All displacements are negative.

† Number of line-images measured.

were blended on most of the plates; for this reason they were seldom observed separately.

Measured displacements of dark lines on the early plates are in Table I, which is complete for component I and also includes data for component II from plates on which both components are visible. The values, all negative, are corrected only for the orbital motion and rotation of the earth (i.e., reduced to sun). To obtain displacements referred to the center of the nova, the correction $-V_n$ must be applied, where V_n is the relative radial velocity of nova and sun.[2] The data of Table I are plotted in Figure 1.

[2] Since V_n is probably about -4 km/sec, the values in Table I are to be diminished numerically by 4.

Further measurements of component II are in Table II (plotted in Fig. 2). These lines, narrow and well defined, like those of component I, are measurable with accuracy over a considerable period.

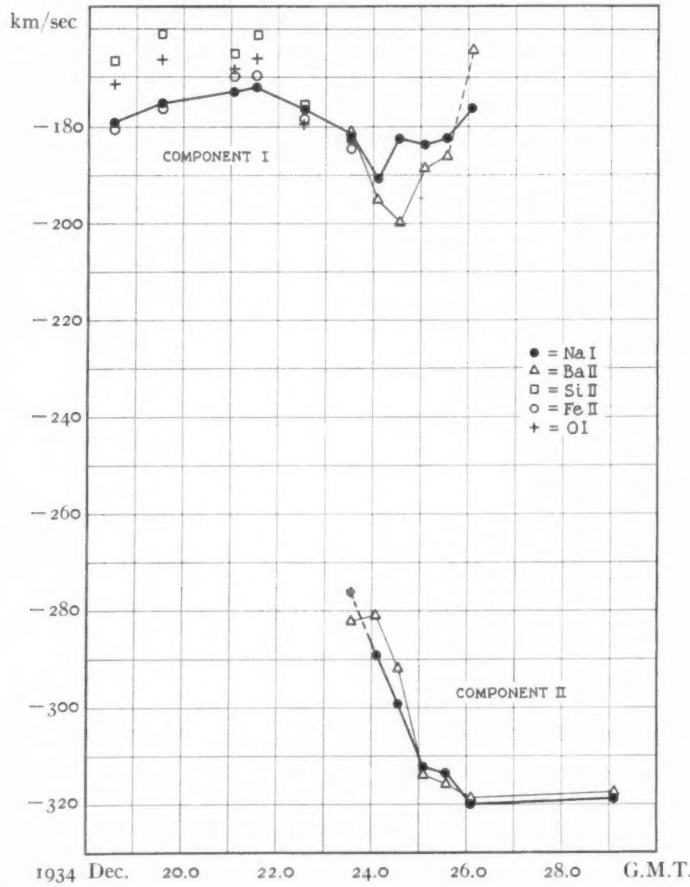

FIG. 1.—Displacements of absorption lines. Component I complete, with the beginning of component II.

A few notes on their behavior will be found in a later section of this contribution.

Many spectrograms show absorption components of sodium and

TABLE II

DISPLACEMENTS OF ABSORPTION LINES IN KM/SEC
(Component II)

G.M.T.	D1, 2	*Sc* II	*Ti* II	*Fe* II	*Si* II	*Ba* II	Misc.
1934 Dec. 29.09 . .	319* 6†	309 2	330 2	. . . . .	307 6	317 3	
30.09 . .	322 12	315 11	322 20	328 11	306 4	311 10	309 3 *O* I, *Cr* II, *Y* II
31.09 . .	319 12	311 3	322 22	322 22	306 8	314 9	311 8 *O* I, *Cr* II, *Y* II
1935 Jan. 3.06 . .	(327) 2	312 8	314 1	315 1	(324) 1	312 3	314 1 *Y* II
12.06 . .	322 12	310 12	324 20	323 15	304 2	311 4	309 3 *Cr* II, *Y* II
16.06 . .	331 8	309 5	326 12	332 9	. . . . .	322 1	313 2 *Cr* II, *Y* II
17.06 . .	330 5	315 8	318 17	328 14	318 2	299 1	314 2 *Y* II
20.05 . .	328 12	314 14	320 13	329 14	. . . . .	315 1	316 3 *Cr* II, *Y* II
21.06 . .	327 8	326 1	331 1	332 8			
25.04 . .	327 2	327 1	. . . . .	324 2			
26.02 . .	330 2	. . . . .	. . . . .	. . . . .			
29.06 . .	345 10	330 3	331 2	347 3			
31.05 . .	338 7	. . . . .	. . . . .				
Feb. 2.05 . .	346 5	339 1	349 2				
11.01 . .	352 3	. . . . .	. . . . .				
15.03 . .	384 6	. . . . .	. . . . .				
16.00 . .	388 3	343 1	. . . . .				
16.97 . .	385 3	. . . . .	. . . . .				
18.00 . .	380 10	371 1	. . . . .				
19.01 . .	383 13	. . . . .	363 3				
Mar. 5.02 . .	384 8	. . . . .	370 2				
17.04 . .	390 4						
20.02 . .	389 3						
21.95 . .	396 2						
23.03 . .	391 1						
25.00 . .	395 13						

* All displacements are negative.

† The number of line-images measured.

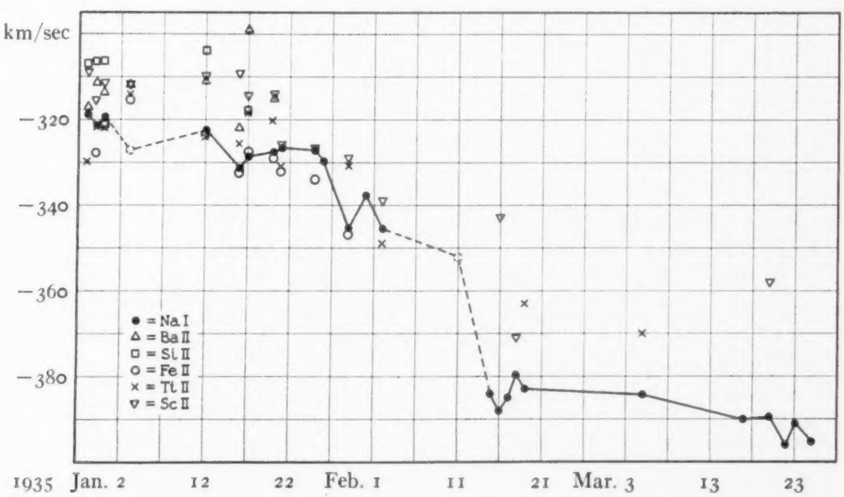

FIG. 2.—Displacements of absorption lines. Component II

other elements with displacements of from 650 to 930 km/sec (Table III). Most of these are wider and more diffuse than components I and II, and accordingly are measurable with much less accuracy.

TABLE III

ABSORPTION COMPONENTS WITH LARGE DISPLACEMENTS, KM/SEC

G.M.T.	D1, 2	*Si* II	*O* I	*Fe* II	*He* I
1934 Dec. 31.09	695* 1†	...	...	...	...
1935 Jan. 12.06	?	700: 2	680: 2	630: 7	704 5
16.05	574 2 692 4	700: 2	707: 1	702 6	...
17.06	570 2 674 2	638: 2	666: 1	660 7	796: 1
20.05	692 4	788 3	801 6	768 13	...
21.06	667 3	746 4	763 2	... ..	... ..
25.04	... ..	... ..	883: 1	... ..	... ..
26.02	... ..	858: 2	... ..	... ..	... ..
29.06	880 6	845: 4	882 3	882 2	788: 1
31.05	871 6	... ..	... ..	... ..	... ..
Feb. 2.05	773 2 877 4	... ..	852: 1	899: 1	... ..
15.02	749 5 918 3	... ..	... ..	... ..	... ..
16.00	757 5 919 3	... ..	... ..	773 4	... ..
16.98	776 2 928 1	886: 2	902: 1	... ..	... ..
18.00	765 4 880 4	... ..	... ..	782 8	... ..
19.02	777 4 904 4	... ..	... ..	790 5	... ..
Mar. 5.04	852: 4	... ..	... ..	833 1	... ..
17.06	... ..	... ..	... ..	860 1	... ..
19.99	... ..	... ..	... ..	... ..	499 1
21.98	... ..	... ..	... ..	... ..	473 2
25.00	614? 1 852 2	... ..	... ..	441 2 858 2	450 3 995? 3

* All displacements are negative. The values followed by a colon are very uncertain.

† Number of line-images measured.

Two components of the sodium lines on plates taken in February are, however, quite narrow and sharp.

A weak component of D2, displacement about −700 km/sec, was seen on December 31.1, 1934, and by January 12.1, 1935, had de-

veloped considerable intensity. On the latter date, corresponding components were measured for lines of *O* I, *Si* II, and *Fe* II. The average displacement on January 12, 16, and 17 was −670 km/sec. On January 20, the lines were stronger and their displacements about 100 km/sec greater. On January 20 and 21, at least two narrow components were probably present within the very broad and intense sodium absorption. By February 2.05 two distinct components had emerged from the complicated line structure, which were measured on numerous plates from that date until February 19.02. On February 2 the component with greater displacement had about three times the intensity of the other, but from February 15 to 19 it was the less intense of the two. It will be recalled that the relative intensity of components I and II changed in the opposite way, i.e., component I, having the smaller displacement, was at first stronger, and later weaker than component II.

EMISSION LINES

The emission lines associated with component I of the absorption spectrum were of the P Cygni type, sharply bounded on their violet edges by the absorption components, but slightly diffuse on their red edges, and had total widths corresponding to about 320 km/sec. With the exception of *H*α they were not of high intensity. Displacements of their effective centers from a few measures, not of high accuracy, on plates taken between December 18.5 and December 23.5 are:

Fe II......	−20 km/sec	*Na*..........	−9 km/sec
O I........	(+16)	*H*α..........	+7
Si II......	−15		

The most conspicuous bright lines associated with absorption component II, in addition to *H*α, were those of *Na*, *Fe* II, and [*O* I]. Extensive data have been obtained for lines of iron and oxygen. Because of the overlapping of D1 and D2, it was not considered profitable to measure sodium emission. A few measures were made on bright lines of low intensity assigned to *Ti* II and *Sc* II. λ 5755 [*N* II] became prominent on the later plates, but its relationship to component II is not clear.

The structure of the bright lines of component II was quite differ-

ent from that of the lines of component I. Their widths were greater throughout, increasing from 540 km/sec to 700–800 km/sec. At first the lines were flat-topped with well-defined edges (profiles rectangular); next they sagged in the middle and became saddle-shaped; finally the maximum on the violet side of the center of the line became much more intense than the red maximum (Plate XIX).

In measuring the lines, settings were made on the edges[3] as well as on the maxima, when these features were well defined. When the lines were nearly symmetrical, additional settings were made on the estimated center of the structure as a whole; and when they were unsymmetrical, the micrometer wire was placed halfway between the unequal maxima. In determining the displacement of each line as a whole, all available settings were combined, although those on edges and maxima were usually given more weight than the bisection settings.

The mean displacements of the emission lines most frequently measured are in Table IV. Although numerous settings of the micrometer wire were made on each line, the accuracy of measurement does not equal that attained on narrow, sharp lines. This is partly because during the period of observation, when the spectrum was complicated, the measurement of a number of lines was interfered with by the superposition and overlapping of various bright and dark lines. The dispersion shown by the displacements of the metallic lines at least is, therefore, not unexpected, although some special circumstance seems to have affected the strong iron lines λ 5169 and λ 5316.

In the case of the [*O* I] lines, however, the differences in velocity, although small, may, because of the large number of measures involved, possibly be significant. The wave-length of the green auroral line, 5577.34 A, has been reliably determined by Babcock and other observers and cannot be greatly in error. The wave-length of the red line 6300.32 A, measured with an interferometer by L. Harang and L. Vegard,[4] gives in Nova Herculis nearly the same displacement as

[3] In spite of attempts to allow for photographic spreading, very intense images were usually measured a little wider than weaker ones; but in general the errors due to varying image density appear not to be large.

[4] *Nature*, **135**, 542, 1935.

that obtained from the green line. Two facts suggest that the adopted wave-length of the second red line,[5] 6363.88 A, may be too

TABLE IV

MEAN DISPLACEMENTS OF EMISSION LINES

I.A.	Displacements	No. of Images
	km/sec	
Fe II 5169.03	*	....
97.56	−0.1	10
5234.62	5.4	9
76.01	0.2	8
84.11	3.6	2
5316.62	†	....
62.11	0.7	10
5534.84	8.9	7
5991.36‡	17.0	23
6084.10‡	16.2	6
6238.39	0.3	4
47.56	3.3	13
6416.92	6.8	9
32.69	21.4	9
56.39	3.7	23
6516.08	−9.6	16
Mean	-7.3 ± 1.2	149
Ti II 5129.17	−9.6	2
5381.02	20.5	4
Sc II 5684.20	17.0	3
[*O* I] 5577.34	19.2 ± 0.7	28
6300.32	21.0 ± 0.4	71
6363.88	-25.0 ± 0.6	34
Mean	−21.5	133
[*N* II] 5755.0	−24.7	4

* On December 30 and 31, 1934, the displacement appeared to be +94. km/sec; in March, 1935, +12. km/sec.

† On December 30 and 31, 1934, the measured displacement was +10.6 km/sec; in March, 1935, −7.2 km/sec.

‡ λ 5991.36 and λ 6084.10: These appear to be the leading lines of a new *Fe* II multiplet, $a^4G - z^6F^o$, recently calculated by Miss Charlotte E. Moore, to whom I am indebted for an opportunity to use the data before publication.

great by about 0.1 A: (1) if it were reduced by this amount, the resulting displacement in Nova Herculis would equal that obtained from λ 5577 and λ 6300; (2) if the interval $\Delta\nu = 158.13$ between the $^3P_2$ and $^3P_1$ levels, determined by Hopfield[5] with high dispersion

[5] J. J. Hopfield, *Phys. Rev.*, **37**, 160, 1931.

from the ultra-violet lines 1302.185 A and 1304.872 A, be applied to the line 6300.32 A, the computed wave-length is 6363.74 A.

Measurements of the bright lines of *Fe* II and [*O* I] included in Table IV are grouped according to date in Table V. "Displacements" are of the centers of the lines, determined in the manner previously described. The columns headed "$W/2$" give the half-

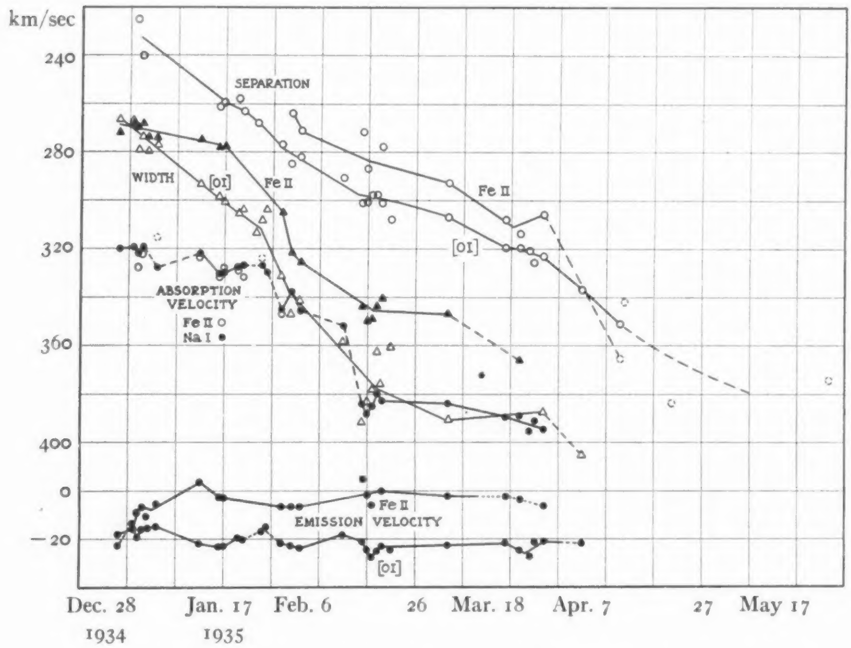

FIG. 3.—Data concerning emission lines, with displacements of absorption component II for comparison.

distances between the outer edges of the lines, while under "$S/2$" are the half-distances between the points of maximum intensity. These data are plotted in Figure 3.

The displacement of the iron lines seems to have increased (in the algebraic sense) progressively from December 26, 1934, to January 12, 1935. Thereafter the apparent fluctuations probably do not exceed the errors of observation. The mean velocity for the first six dates is −10.5 km/sec, with a probable error, if the true velocity

is assumed to be constant, of ± 1.2 km/sec, while that for all the remaining dates is -3.5 ± 0.7 km/sec. Comparable values from the

TABLE V

MEASUREMENTS OF EMISSION LINES, KM/SEC

G.M.T.	*Fe* II						[*O* I]					
	Displ.		*W*/2		*S*/2		Displ.		*W*/2		*S*/2	
1934												
Dec. 26.09	−18.4	4*	272	4	...	..	−22.3	1	266	1	...	..
29.09	−16.0	16	268	16	...	..	13.8	3	267	3	...	..
30.09	− 9.3	38	270	38	...	..	19.5	7	279	7	225	1
31.09	− 6.6	24	268	28	...	..	16.2	6	274	6	240	1
1935												
Jan. 1.06	−10.4	3	274	8	...	..	16.0	1	280	3	...	..
3.06	− 5.8	4	274	4	...	..	15.2	7	277	3	...	..
12.06	+ 3.7	7	275	9	...	..	22.0	3	294	4	...	..
16.07	− 2.4	2	278	2	...	..	23.6	4	299	4	261	3
17.06	− 2.9	9	278	9	...	..	23.0	7	301	7	260	5
20.05	...	..	...	..	...	..	19.3	3	306	4	258	2
21.07	...	..	...	..	...	..	20.3	3	304	3	263	3
24.01	...	..	...	..	...	..	...	..	314	3	268	2
25.04	...	..	...	..	...	..	17.1	1	308	1	...	..
26.02	...	..	...	..	...	..	15.4	1	304	1	...	.
29.06	− 7.2	7	305	7	...	..	21.7	5	330	5	277	6
31.05	− 7.1	16	322	12	264	6	23.0	7	348	7	285	6
Feb. 2.04	− 7.3	9	326	9	271	4	23.9	5	341	5	282	3
11.02	...	..	...	..	...	..	18.7	3	359	3	291	2
15.00	+ 4.4	2	344	1	272	1	20.9	6	392	6	301	5
16.01	− 2.3	4	350	4	287	4	24.3	3	383	3	301	3
16.98	− 6.2	1	349	1	...	..	27.4	4	378	4	298	4
17.99	...	..	344	1	...	..	25.4	7	363	7	298	7
19.00	− 0.3	4	341	4	278	1	22.9	11	376	10	301	8
21.02	...	..	...	..	...	..	24.7	2	361	2	308	2
Mar. 5.02	− 2.3	7	347	6	293	7	23.0	7	392	3	307	7
17.04	− 2.8	1	...	..	308	2	22.1	5	...	..	320	5
20.00	− 3.9	2	367	1	314	2	25.1	3	...	..	320	3
21.97	...	..	...	..	...	..	27.9	3	...	..	321	3
23.03	...	..	...	..	...	..	21.2	2	...	..	326	2
25.00	− 6.4	2	...	..	306	4	21.2	11	388	5	323	11
Apr. 2.00	...	..	...	..	...	..	22.2	2	406	1	338	2
9.97	...	..	...	..	366	1	(11.2)	1	...	..	351	2
11.03	...	..	...	..	...	..	...	..	...	..	(342)	1
20.94	...	..	...	..	...	..	...	..	...	..	384	1
May 23.92	...	..	...	..	...	..	...	..	...	..	(374)	1
Mean	(− 6.4±0.8)		...	..	...	..	−21.4±0.4		...	..	...	..

* Number of line-images measured.

[*O* I] line λ 6300.32 are -17.4 ± 0.8 km/sec and -22.0 ± 0.4 km/sec, respectively, indicating a small change in the opposite direction.

A few comments on the widths of the emission lines and the distances between their maxima listed in Table V will be found in the discussion.

NOTES ON THE BEHAVIOR OF LINES OF VARIOUS ELEMENTS

An idea of the times of occurrence of the lines of certain elements may be gained from Tables I, II, III, and V. Additional information concerning the intensities of bright and dark lines is furnished by miscellaneous comments in the preceding pages and by the following notes.

Sodium.—On several of the very early plates narrow dark lines of low intensity, possibly interstellar, appear near the normal positions of the sodium lines. D2 is clearly seen on a few of the best plates, while D1 is apparently on the threshold of visibility. The approximate displacement is −18 km/sec, in reasonable agreement with the value of −21 km/sec found by other observers[6] for the detached lines of calcium. The detached sodium lines were not measured after the development of component II of the nova absorption lines because the displaced D1 then nearly coincided with detached D2 and was of far greater intensity.

Ionized barium.—The lines measured, in absorption only, are λλ 5853.70, 6141.74, 6496.91. Components I and II, although both had been weak or absent on December 22.5, suddenly appeared on December 23.5. Component II was the less intense; but on December 24.1, only half a day later, it had gained noticeably in intensity; on December 24.5, it was approximately equal to component I; and on December 25.1 it was the stronger. On December 26.1, component I was barely measurable, while component II increased in intensity until December 29, after which it declined, being last measured on January 20. Throughout their relatively brief apparition the lines of both components were narrow. Their relative intensities ran a course nearly parallel to that of the sodium lines, although the two components may have reached equal intensity half a day earlier than those of sodium.

Oxygen.—Many observers have commented on the conspicuous presence of dark lines of neutral oxygen during the early period.

[6] E. G. Williams, *M.N.*, **95**, 577, 1935; W. S. Adams, W. H. Christie, A. H. Joy, R. F. Sanford, and O. C. Wilson, *Pub. A.S.P.*, **47**, 208, 1935.

The remarkably high intensities of these lines form one of the outstanding differences between the spectrum of the nova at this time and that of α Cygni. The emission borders on the red sides, however, were not very intense. The chief lines observed in the present investigation include

$$\begin{array}{ll} 5958.53 & \left.\begin{array}{r} 6453.69 \\ 54.55 \\ 56.07 \end{array}\right\} \\ 6046.34 & \\ \left.\begin{array}{r} 6155.99 \\ 56.78 \\ 58.20 \end{array}\right\} & \end{array}$$

The lines of oxygen first observed were associated with component I and rapidly decreased in intensity as component II and the cyanogen bands developed. The lines listed above were never conspicuous in component II. Ill-defined components with larger displacements were measured on a number of the later plates (Table III). Emission in the position of the oxygen triplet $\lambda\lambda$ 7772–7774–7775 was observed on February 15.

The forbidden line λ 6300.32, which was emerging in emission on December 25.5, was distinct on December 26.1, and was much more intense on December 29.1 and later. The auroral line λ 5577.34 was well marked on December 30.1, the date of the first grating spectrogram of the green region. The later behavior of these lines will be described in another contribution.

Enhanced iron.—In the green and red regions of the spectrum of Nova Herculis, numerous enhanced iron lines were conspicuous through a considerable interval of time. Absorption component II was measured until about the last of January (Table II), while components of larger displacements were observed over a much longer period (Table III).

Table IV lists the emission lines observed. They were emerging on December 25.1, slightly in advance of λ 6300 [*O* I], and were distinct on December 26.1, becoming much more intense on December 29 and 30, but declined slightly on December 31 about the time of light-maximum. On January 12, 16, and 17 the iron emission lines were much less intense. These lines were not measured from January 20 to January 26, although a few of the strongest were present. They became more distinct toward the end of January, after which

the intensity again declined; but the strongest lines remained visible for many weeks (Table V).

Enhanced titanium.—A number of absorption lines, chiefly in the green, were measured regularly from December 29.1, the date of the first suitable plate of the green region, to about January 20, and on a few plates thereafter. These lines associated with component II were well defined. They included

5129.17	5211.58	5336.78
54.07	26.56	81.02
83.73	62.14	5418.77
85.90	68.63?	6491.68
88.70		

The emission components were relatively weak and in the complex spectrum were recognizable with certainty only where favorably situated. About the end of December, a few measures were made on λ 5129.17 and λ 5381.02.

Ionized scandium.—A number of well-marked absorption lines, of which λ 5526.82 and λ 5657.88 were conspicuous, appeared on the early plates of the green region. The lines belonged to component II and were narrow and sharp. Lines measured in the green and red include

5239.81	5669.59
5526.82	84.20
5640.99	6245.63
57.88	79.74
67.16	6604.61

The intensity, which appeared to increase in the twenty-four-hour interval December 30.1 to December 31.1, remained high until about January 20. After that date these lines faded rapidly; by January 31 they were very much less intense, but a trace of the two strongest persisted at least until February 19.

Emission components, if present, were of very low intensity. A bright line, measured on a few plates taken toward the end of December near the normal position of *Sc* II 5684.20, is ascribed to that line.

Ionized yttrium.—The behavior of λ 5662.94 is very similar to that of lines of *Sc* II.

Helium.—During the latter part of March, absorption D3 was

well marked; but on most of the earlier plates it was either absent or too weak and ill-defined for measurement. Table III records the few measured displacements considered of any value. Emission, while clearly present on numerous spectrograms, is too badly mutilated by displaced sodium absorption to be measurable for displacement. Photometric tracings may later make possible a better description of the behavior of the emission and absorption components.

Ionized nitrogen.—The behavior of the forbidden line λ 5755.0 was somewhat similar to that of the forbidden lines of neutral oxygen, but the structure was wider and the edges and maxima were not nearly so well defined. The line (in emission only) emerged so gradually from the continuous spectrum that the date of its first appearance is uncertain, but it seems to have been definitely present on January 21. Thereafter it grew stronger, although with some fluctuations in intensity. The maximum of shorter wave-length stood out strongly on April 10, April 21, and May 24. On most plates measures were very difficult, but the mean displacement agrees within the error of determination with that yielded by the [*O* I] lines (Table IV). The mean value of the half-separation of the maxima for March 5, 17, 20, 25, and April 10 was 400 km/sec, while the corresponding value for the [*O* I] lines varied from 307 to 351 km/sec.

DISCUSSION

An adequate discussion of the data recorded in the foregoing pages would take us deep into the unsolved problems of temporary stars and would properly involve a comparative study of much other material. This should obviously be undertaken at some future time when numerous other investigations of Nova Herculis have been published. The writer will therefore conclude the present contribution with a few brief comments, leaving to others the larger task of assembling and co-ordinating measurements made in other parts of the spectrum, as well as the more interesting one of intercomparing the spectroscopic phenomena of various novae. It is hoped later to publish microphotometric tracings of certain features whose widths and displacements have been dealt with in the present investigation.

The hypothesis of an expanding atmosphere, introduced by Halm[7] many years ago, and now generally adopted as a working hypothesis

[7] *Proc. Roy. Soc. of Edinburgh*, **25**, 513, 1904.

to account for the spectroscopic phenomena of novae, may take one of two general forms in which the simplest cases are:

a) The instantaneous emission (from the body of the star) of atoms which travel outward as a thin shell of ever increasing radius.

b) The continuous emission of atoms which are spectroscopically active only in a thin stratum at a fixed (or *slowly* changing) distance above the photosphere.

For observations at a given instant or within a sufficiently small interval of time, (*a*) and (*b*) might be indistinguishable. More complicated cases would include the emission of many successive shells, or a condition in which there was spectroscopic activity throughout a thick layer of gas surrounding the photosphere. To make the hypothesis still more flexible, various observers have postulated a non-spherical distribution of velocities such as would be caused by rotation or by jets of matter sent out from localized areas.

It is well known that various dark lines yield essentially the same displacements (outward velocities) regardless of the weight or electrical charge of the atoms to which they are due. For example, in the present measurements, the displacements of lines of barium (atomic weight 137) are very similar to those of sodium (atomic weight 23) and do not differ greatly from those of lines of yttrium (89), scandium (45), or oxygen (16). Small systematic differences between certain groups of lines do exist, however, as has been pointed out by W. S. Adams *et al.*[8] The last column of Table VI is taken from measurements at Mount Wilson of numerous lines in the "photographic" portion of the spectrum.[8] Comparison with the preceding column shows that on corresponding dates the values for sodium (D lines) differ by about 10 km/sec. See also Tables I and II, or Figures 1 and 2, for other instances of small differences.

Results for the widths and displacements of the emission lines, plotted in Figure 3, show that although the widths increased greatly, the centers remained very nearly in their original positions. In other words the lines underwent a symmetrical expansion about their normal places.[9] This fact, taken in connection with the

[8] *Pub. A. S. P.*, **47**, 206, 1935.

[9] This statement neglects the decreasing relative *intensities* of the redward halves of the lines.

parallelism of the width-curve with that showing the increasing displacement of the dark lines, is favorable to Halm's hypothesis. One interesting implication is that the behavior of the edges of the lines is not dependent on their limitation by contiguous absorption. In the iron lines, the red edge, where no absorption has been observed, moved away from the center just as did the violet edge, while in the forbidden lines there is, of course, no absorption at either edge.

TABLE VI

SUMMARY OF MEASUREMENTS

(Values in Km/Sec)

Date	Emission									Absorption	
	[*O* I]			*Fe* II			[*O* I]-*Fe* II			*Na*	*Fe* II *Ti* II, Etc.
	Displ.	*W*/2	*S*/2	Displ.	*W*/2	*S*/2	Displ.	*W*/2	*S*/2	Displ.	Displ.
1934											
Dec. 29	−16	270	.....	−16	270	.....	0	0	.....	−320	−310
Dec. 31	16	274	240	10	270	.....	− 6	4	.....	320	310
1935											
Jan. 16	22	300	260	2	277	.....	20	23	.....	330	321
Jan. 31	22	338	282	7	318	266	15	20	16	342	334
Feb. 17	24	(376)	300	2	344	282	22	(32)	18	384	362
Mar. 5	23	(390)	307	2	(353)	293	21	(37)	14	384	(371)
Mar. 22	−24	(388)	322	− 4	(362)	310	−20	(26)	12	−393	−385

Similarly, the behavior of the maxima points toward a real (geometrical) symmetry of some kind, for these features are *within* the emission, and settings on them could not be greatly influenced by the absorption components. The ratio, width to separation, is about 1.2 for permitted and forbidden lines alike.

We must not forget, however, that Halm's hypothesis does not directly account for *accelerated* motion such as that observed in the atmosphere of Nova Herculis.[10] In form (*a*), page 428 (which seems

[10] While the accumulated change in the observed velocity was considerable, the actual acceleration per second was moderate. Its largest value, apparently on December 24, was about 50 times that of solar gravity at the distance of the earth and not much more than 1/1,000 that at the surface of the sun.

to be the usual interpretation), the velocity should apparently either remain constant or decrease slightly because of the gravitational attraction of the star on the receding atoms. Light pressure, however, or some other force which acts outward, is evidently more effective than gravity. On hypothesis (*b*), since successive observations deal not with the same atoms, as in (*a*), but with atoms emitted at different times, we must assume that the increasing velocities correspond to slightly different circumstances of emission.

The comparative behavior of the lines of *Fe* II and of [*O* I] is interesting. At first the widths were the same, as were also the displacements; but after December the [*O* I] lines had the greater widths and separations, and their centers were displaced about 20 km/sec to the violet with respect to those of the *Fe* II lines. The differences may tentatively be explained on Halm's hypothesis as follows: Both lines will have the same redward limit, namely, that corresponding to the radial velocity of the points C and C', Figure 4, while the violet edges of the permitted lines will correspond to the points A and A', but those of the forbidden lines, to the greater negative velocity at O. It is easily seen that the difference of the half-widths should equal the difference of the displacements of the centers, and Table VI shows that this relationship is approximately fulfilled. The last three values of the differences of width are probably too large, because the [*O* I] lines were more intense than the *Fe* II lines and were thus measured relatively too wide. Better values for comparison with the differences of displacements might be obtained by increasing by one-fifth the differences of the separations.

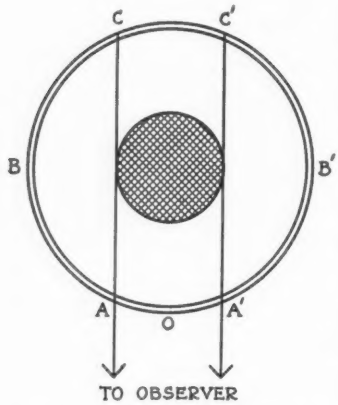

FIG. 4.—Halm's expanding-shell hypothesis.

If the foregoing reasoning is correct, the radial velocity of the center of Nova Herculis is that yielded by the permitted lines, about -4 km/sec. Moreover, we can compute the relative radius R of the

gaseous shell in terms of that of the photosphere. The width of permitted lines is $V \frac{2\sqrt{R^2-1}}{R}$, where V is the actual velocity of expansion of the shell (given in close approximation by the absorption lines plus correction for motion of the center of the nova), while the width of forbidden lines is $V\left(1+\frac{\sqrt{R^2-1}}{R}\right)$ and the difference Δ is $V\left(1-\frac{\sqrt{R^2-1}}{R}\right)$. If we take $\Delta=40$ km/sec and $V=340$ km/sec, R is found to be 2.1. In other words, the absorbing and emitting shell has twice the radius of the photosphere.

The conclusions in the preceding paragraph must be accepted with reserve. Two curious facts tend to weaken our confidence in them. One is that at the end of December the widths and displacements of the *Fe* II lines agreed with those of [*O* I]; the other is that the forbidden line λ 5755 [*N* II] had a greater width than the [*O* I] lines. Hence, effects other than those of the simple Halm hypothesis appear to be active.

To explain the common outward motion of numerous atoms of various kinds, and also the fact that this motion is far greater than the kinetic velocities of the gaseous atoms, we may appeal to light-pressure[11] acting in a layer having the requisite viscosity[12] to prevent rapid separation of the atoms; or we may imagine that an explosive pulse originating below the photosphere drives off a layer of material in a condensed or quasi-liquid state from which, after the driving force has ceased, the atoms quickly evaporate into a normal (spectroscopically active) gas, retaining by inertia their high systematic outward velocities. This hypothesis, which appears to be in accord with certain observed facts, would probably find its best test in the very early stages of nova history.

Carnegie Institution of Washington
Mount Wilson Observatory
September 1935

[11] E. A. Milne, *M.N.*, **86**, 466, 1926.

[12] W. H. McCrea, *ibid.*, **95**, 509, 1935.

NOTES

NOTE ON THE PHYSICAL SIGNIFICANCE OF THE n AND s CLASSIFICATION OF A STARS

In a recent paper Struve suggests that rapid stellar rotation should produce a spurious absolute-magnitude effect.[1] Thus, if a star with no rotation should in some way be given a high rate of rotation, the spectral lines would take on the characteristics of a star with a higher level of ionization, owing to the great decrease in surface gravity caused by the high centrifugal force. In addition, of course, the lines would be broadened. He calls attention to the Adams and Joy classification of B and A stars,[2] in which the more luminous stars in a given spectral subclass have sharper lines than the less luminous ones (excluding the *H* and *Ca* II lines). Thus, the absolute magnitude of an A2s star is $+0.9$ and that of an A2n star is $+1.7$, as given by Adams and Joy.

Struve concludes that, unless systematic errors are present in the classification, either the more luminous stars rotate more slowly than the less luminous ones or the decrease in surface gravity due to the rapid rotation of the less luminous star makes it appear to belong to an earlier spectral class than it would if it had no rotation. If the second assumption is correct, the effective temperature of the A2n star should be lower than that of the A2s star.

Now there is strong evidence that this is the case, as is shown in the accompanying data taken from Table VII of *Harvard Circular* 348 by the writer. The third and seventh columns contain the mean color equivalent, which is simply a constant divided by the temperature. It is seen that the average temperature of an A2n star is equal to that of an A5s star and that its absolute magnitude, M, is also about the same. In fact, if the data in the right-hand side of the table are moved down three lines, the agreement between the cor-

[1] *Pop. Astr.*, **43**, 496, 1935.

[2] *Mt. Wilson Contr.*, No. 244, 1922, and No. 262, 1923.

responding values of M and C_2/Temp. on the two sides of the table is very good.

Adams and Joy		Mean Value of C_2/Temp.	No. of Stars	Adams and Joy		Mean Value of C_2/Temp.	No. of Stars
Class	M			Class	M		
B9s	−0.2	1.56	2	B9n	+0.5	1.64	4
A0s	+0.2	1.58	1	A0n	0.9	1.67	8
A1s	0.6	1.57	3	A1n	1.3	1.67	9
A2s	0.9	1.62	7	A2n	1.7	1.82	6
A3s	1.2	1.72	3	A3n	2.0	1.89	2
A4s	1.6	1.73	2	A4n	2.2	2.08	3
A5s	+1.8	1.82	2	A5n	+2.3	2.13	2

It seems fairly safe to conclude, then, that the n stars do indeed show a higher level of ionization than they would show if they had no rotation.

Emma T. R. Williams

Leander McCormick Observatory
University of Virginia
October 22, 1935

MICROMETRIC OBSERVATIONS OF NOVA HERCULIS

ABSTRACT

The separation of the components of Nova Herculis has increased at the rate of about $0\overset{''}{.}27$ per year since July, 1935. The difference in magnitude, about $0\overset{M}{.}5$, has remained approximately constant.

Since Dr. Kuiper's announcement, on July 4, of the duplicity of Nova Herculis, the relative position of the two components has been measured at the Yerkes Observatory whenever conditions permitted. The measures secured to date are given in Table I.

During the 0.34 year, now covered, there is no evidence of a change in the position angle or in the relative magnitude, but there has been a steady increase in the distance. Other observers have made the separation larger than the foregoing during the first month; but the difference is not larger than the customary personal equation in close pairs, the more so because of the unusual appearance of the star. The visually dominant part of its light being the emission near λ 5000, the star presents a strikingly green color as seen in the

40-inch refractor. When the telescope is focused for that wavelength, the two nuclei appear vividly green with starlike disks of the normal diffraction diameter. If we change the focus to the region of λ 5800, the components become small yellow nuclei surrounded by the out-of-focus green halo. These nuclei appear sharper and smaller in diameter when seen in the yellow than when seen in the green, and, while the black space between the components appears larger in the yellow than in the green, the separation of the components from center to center is not appreciably different.

TABLE I

	Angle	Distance	ΔM
1935.511	124°6	0″16	....
.514	127.2	.15	....
.519	134.0	.18	....
.544	125.1	.17	....
.566	129.2	.18	$0^{M}5$
.622	124.9	.16	....
.678	128.8	.18	.6
.766	128.6	.19	....
.812	130.4	.21	....
.851	129.0	0.23	0.6

It is probable that the two components started separating at the time of the first outburst of the Nova last December. If so, the measures indicate a rate of separation of about 0″27 per year, if uniform. This corresponds to a relative velocity in km/sec of 1″3 divided by the parallax. Assuming 0″002 for the latter, this velocity would be of the order of 600 km/sec. It is also probable that, whatever the nature of the two components, we are dealing with matter ejected in opposite directions from a center of mass, not now shining in emission light like the two components and therefore overshadowed by their green emission. The velocity of ejection would, therefore, have been of the order of 300 km/sec, which is in fair agreement with direct spectroscopic evidence. The remarkable constancy of the light of the Nova during these last months has been of great advantage in establishing the change in the separation of the components.

G. Van Biesbroeck

Yerkes Observatory
November 19, 1935

REVIEWS

The Rise of Modern Physics. By HENRY CREW. 2d ed. Baltimore: Williams & Wilkins, 1935. Pp. xvii+434. $4.00.

Students of the physical sciences have difficulty in finding time to include in their college work a course in the history of physics. It is perhaps for this reason that there are graduate research workers who regard the whole of nineteenth-century physics as little more than a moldy ruin contributing little to the quantized if somewhat indeterminate structure now being reared in its stead.

Such a lack of historical perspective can in large degree be remedied by the study and enjoyment of Professor Crew's concise yet inspiring account of the creation of the main body of present-day physics. Since it was part of his purpose "to reduce to a minimum the accounts of mistaken viewpoints and outworn theories," he merely summarizes the more fruitful conceptions of ancient and medieval physics, devoting the greater part of the book to the three centuries from the time of Galileo to the introduction of quantum mechanics. He is here concerned primarily with the development of vital ideas; by the elimination of unrelated details he is able to emphasize the connections between discoveries widely separated in time and place and thus to unify his subject.

The second edition differs from the first through numerous slight changes in the text and the addition of new chapters covering the origin of modern electrical units, the inertia of electricity, and restricted relativity. Like many of the earlier chapters, these discussions contain so much sound physics that they can serve well as general introductions to the study of these branches of the subject. In particular, the description of the gradual systematization of electrical units should clarify the ideas of more than one bewildered student.

Finally it should be said that the author's unassuming scholarship lends to the work rather the flavor of a stimulating essay than the drier taste of a textbook.

P. C. KEENAN

Relativity, Thermodynamics and Cosmology. By R. C. TOLMAN. Oxford: Clarendon Press, 1934. Pp. xv+502, with 13 figures. $8.50.

In 1930 the significance of the non-static solutions of the Einstein field equations for cosmological questions was generally recognized and the

interest of physicists and astronomers in the theory of relativity increased so much that an adequate treatment of the recent developments within the frame of the whole theory became necessary. R. C. Tolman was especially competent for this task, since he himself had made a great many important contributions to the theory since its early days.

Tolman's book presents the theory in two large sections; the first of which treats the special theory (chaps. ii–v), while the second is devoted to the general theory (chaps. vi–ix). Each of these sections begins with the fundamental principles, continues with mechanics and electrodynamics, and ends with thermodynamics. Chapter x, giving the applications to cosmology, fills about one-third of the whole book.

Aside from the thermodynamical and cosmological discussions, the treatment of the older parts of the theory naturally coincides in many ways with the respective treatments of other authors. Special reference is made to Eddington's well-known book. But in other respects the dynamics of continuous mediums is developed to a greater extent than usual, in order to prepare the reader more carefully for the chapters on thermodynamics.

The equivalence of energy and mass is the most important contribution of relativity to thermodynamics. Tolman deals with it in the first part of chapter v, which opens with an introduction to the foundations of classical thermodynamics. The second part of the chapter contains the thermodynamics of moving systems and its four-dimensional Lorentz-invariant formulation as a preparation for the general-invariant formulation in the first part of chapter ix, which later allows the incorporation of any gravitational fields into thermodynamic systems. The second part of chapter ix deals with important applications. The postulate of stationary entropy serves as the definition of states of equilibrium. From this postulate the conclusion can be drawn that in static systems which are in thermal equilibrium the proper temperature is not constant, but depends on the gravitational potential. This can easily be seen if one considers that according to the theory of relativity any form of energy (including heat) is gravitating. Hence there is formed a current of heat which in cases of equilibrium must be compensated for by a temperature gradient. Moreover, some of the most surprising thermodynamical possibilities are shown which are connected with non-static solutions of the field equations. For example, the models which are described by these solutions may undergo finite variations of state in a finite time, whereas the entropy remains constant.

The treatment of the static cosmological models in the first part of chapter x follows well-known standards. The second part deals with the

non-static line elements which are introduced with a very general motivation. After the usual specialization toward homogeneous and isotropic models, the mechanical and optical conclusions are drawn. The third part appears to be one of the most important of the book. It contains, on a large scale, an application of the general-invariant thermodynamics to which the author himself has contributed so greatly. The cosmological considerations come to their end and find their conclusion in the fourth part. The introduction describes very cautiously the viewpoint of the author:

> . . . . We have the right to hope that the models can be so constructed as to assist in the correlation and explanation of the observed phenomena of the actual universe, and indeed may even be sufficiently representative as to permit some cautious extrapolation forward and backward in time, which will give us not too fallacious ideas as to the past and future history of our surroundings.

The data of observation and the conclusions drawn therefrom are presented, at first, without any reference to the theory of relativity, mainly in accordance with Hubble's work. Sections 178–185 are the most essential for the application of the theory to reality. They deal with those quantities of the theory which are essentially observable. The considerations of these parts are of a fundamental character, though they may at first sight seem rather simple. Shortly before the appearance of Tolman's book the manner of applying the theory to the actual universe was in several respects almost uncritical. As a consequence, there appeared at about the same time investigations by De Sitter and by McCrea, which took up nearly the same questions. General considerations regarding the relevancy of the presented models are given with a great deal of reserve at the end of the chapter. An appendix contains symbols, formulae, and physical constants; a subject and name index follows.

Tolman's book may be characterized as follows: It places the greater emphasis on the development of physical concepts rather than on the experimental and mathematical side. Some passages are devoted to the experimental foundations of the special theory of relativity, but for that field the author refers the reader to the literature. The famous effects of the advance of perihelion, the shift of the spectral lines, and the deflection of light are also treated in a somewhat cursory manner. On the other hand, the Riemannian geometry does not explicitly occur in the discussion. The relativistic treatment of atomic questions and the unified field theories are purposely omitted. The omission, however, of a presentation of the highly instructive problems of wave optics is to be regretted. It seems to the reviewer that the theory of the expanding universe would

have been more vivid if it were connected with such a representation. Even such elementary things as aberration and Doppler's principle might have been treated within the special theory as examples of electrodynamics in free space. Doubtless the author has good reasons for these omissions. Still it may be asked whether the strong emphasis of thermodynamics compensates for these omissions. Theoretically, of course, the invariant thermodynamics is very interesting, but is it really relevant for the experiment? Does a physicist need to know how to measure temperatures of gases which have, relative to himself, a high velocity? Or what is the significance of the gravity of heat for the theory of stellar structure?

There is still one more point to which I wish to refer. Homogeneous Euclidian spaces can be filled with uniform matter on the principles of Newtonian mechanics; the expanding universe can be described, up to a certain point, in these classical terms which, in this case, are largely similar to relativistic conceptions. This possibility was shown by the investigations of Milne and McCrea[1] after the appearance of Tolman's book. The merit of Tolman's thermodynamics of non-stationary models is thereby not diminished; but it loses its unique position.

On the whole, Tolman's book selects from the immense field of relativity such sections as best conform to his special interests. These sections are presented very clearly and carefully, and in a refreshing manner. The book is to be recommended as an excellent compendium for scientists working in this field. Any student of relativity will read the book with much profit.

O. Heckmann

Göttingen, Germany

[1] Milne, *Quart. J. of Math.* (Oxford), **5**, 64, 1934; McCrea and Milne, *ibid.*, **5**, 73, 1934. See also Milne, *Relativity, Gravitation and World-Structure* (Oxford), pp. 299 ff., 1935.

INDEX TO VOLUME 82

SUBJECTS

INDEX TO VOLUME 82

AUTHORS